# Observations of the Winter Thermal Structure of Lake Superior

A THESIS
SUBMITTED TO THE FACULTY OF
UNIVERSITY OF MINNESOTA
BY

Daniel James Titze

IN PARTIAL FULFILLMENT OF THE REQUIREMENTS
FOR THE DEGREE OF
MASTER OF SCIENCE

Jay Austin

August 2013

# Abstract

Moored thermistor strings that span the water column have been deployed at up to seven locations throughout Lake Superior from 2005 through present, producing a unique year-round record of the thermal structure of a large lake. This extensive temperature record reveals significant interannual and spatial variability in Lake Superior's winter heat content, thermocline depth, and phenology. Of particular mention is a stark contrast in thermal structure between the cold, icy winter of 2009 and the much warmer winter of 2012, during which especially strong and weak negative stratification was observed, respectively. Significant interannual and spatial variability was also observed in Lake Superior ice cover, as shown through data extracted from Ice Mapping System satellite imagery (NOAA/NESDIS 2004). When water column heat content was estimated from temperature data and analyzed in concert with lake ice-cover data, it was found that ice cover can inhibit heat flux between the lake and the atmosphere, and that spatial variability in ice cover can translate into spatial variability in end-of-winter heat content. Such variability in end-of-winter heat content is found to be preserved through the spring warming season, and is strongly correlated with variability in the timing of the onset of summer stratification, with regions that have warmer end-of-winter water columns stratifying earlier than regions with colder end-of-winter water-columns.

# Table of Contents

# List of Tables

# List of Figures

# 1.0 Introduction

Thermal structure dynamics of large lakes are complex, with external meteorological and climatic forces driving a lake's internal processes. Thermal characteristics of a lake, such as heat content, thermocline depth, and the strength and timing of stratification, are all influenced by interactions between the lake and its surrounding atmosphere. Many important meteorological forces exhibit average annual trends, which ultimately dictate the typical annual thermal structure of the lake. However, the Earth's climate is changing, thus altering these annual atmospheric cycles and, in turn, the thermal properties of the lake. Variations in these forces are expressed in the lake's thermal structure; however, the intricacies of this response are not well-understood. The ability to predict the effects of a changing climate on a lake's thermal composition lie in understanding the mechanisms driving these interactions.

Recent studies have investigated the thermal characteristics of large lakes. Datasets examined in such studies have been obtained using a variety of methods, including direct, in-situ measurements (Austin and Colman 2007; Austin and Colman 2008; Coats et al. 2006; Hampton et al. 2008; Verburg et al. 2003; Vollmer et al. 2005), remote sensing techniques (Schneider et al. 2009; Schneider and Hook 2010), and other sources, such as historic records of ice cover (Magnuson 2000). However, collecting data in large lakes requires overcoming challenges not encountered when making measurements on land, and the establishment of long-term programs to measure lake temperature has only occurred relatively recently, with the earliest known records beginning in the early 20$^{th}$ century (Austin and Colman 2008; McCormick 1996;

McCormick and Fahnenstiel 1999). Wave conditions inherent to large lakes make accessing open-water locations nontrivial. On lakes experiencing seasonal ice cover, access to the open water is generally not feasible during winter months. This has led to a seasonal bias in many long-term lake records, with greater availability of data from summer months than from winter. In addition, most observations of lake temperature are taken at or near the lake surface, with much less documentation surrounding the thermal structure of lakes below the surface.

For those records with sufficient data to elucidate long-term temperature trends, there is a consensus that surface temperatures are increasing at a significant rate. Most of this warming has occurred within the last few decades (Austin and Colman 2008). Although there is great variation in the warming rates presented in studies, such trends have been observed in both tropical lakes (O'Reilly et al. 2003; Verburg et al. 2003; Vollmer et al. 2005) and mid-latitude lakes (Austin and Colman 2007; Coats et al. 2006; Hampton et al. 2008; Schneider et al. 2009; Schneider and Hook 2010). Evidence suggests that warming rates vary as a function of lake geography and morphology (Bennett 1978; Stefan 1998), explaining some of the variation in reported warming rates.

However, due to the complex response of a lake to meteorological variability, there is a great deal of interannual variation superimposed on these long-term trends. As meteorological conditions vary with both diurnal and seasonal signals, lakes are constantly seeking thermal equilibrium with their surroundings. This is especially important for lakes in mid-latitude regions, where annual air temperature signals are much stronger than those of tropical climates. However, a rise in air temperature does

not result in an equivalent increase in lake surface temperature (Roberston and Ragotzkie 1990; Austin and Allen 2011). Rather, the relationship between the temperature of a lake's surface layer and its surrounding atmosphere depends on a multitude of environmental inputs.

While the sensitivity of a lake to some of these inputs, such as air temperature and wind speed, can be modeled using heat flux equations, one-dimensional modeling is not sufficient to fully explain a lake's complex response to these environmental variations. One issue encountered with such modeling is a co-dependency of variables. For instance, a positive correlation has been found between surface water temperature and wind speed (Desai et al. 2009), due to destabilization associated with a weaker temperature gradient at the air-water boundary layer. Further, ice cover has been declining over the last several decades (Assel 2003; Assel 2005; Wang et al. 2012), and such changes to the timing and extent of ice cover certainly have implications for lake-atmosphere interactions (White 2012), but the role of ice cover is difficult to characterize, measure, or model, and remains poorly understood.

In addition, the long-term behavior of lakes below the surface has been largely unexplored. The studies and datasets referenced above were all derived from temperature measurements taken at or near the water surface. While broad generalizations about a lake's annual thermal structure cycle can be drawn from its mixing extent and frequency (Lewis 1983), the physical intricacies of a lake's thermal structure through these cycles are not well documented. This is especially true of large lakes. Characteristic parameters such as heat content, thermocline depth, and the timing and duration of stratification

periods are known to fluctuate from year to year. The mechanisms driving these interannual variations merit additional study, as they have been shown to impact essential biogeochemical processes within lakes (Bennington et al. 2010; White et al. 2012).

Previous work has begun to investigate such characteristic parameters in the context of Lake Superior; however, these studies have had to work around data limitations. Bennett (1978) made estimates of Lake Superior's annual heat content cycle, but the data used was mostly from late April through late November, with winter estimates based on a limited amount of data from mid-December to mid-February. Austin and Colman (2008) estimated the duration of Lake Superior's stratified summer season over the previous 100 years, beginning in 1906, and found it lengthened from 145 days to 170 days over the course of the study period. In their study, the temperature record was derived from measurements taken at a major outflow using an empirical calibration curve, and summer stratification onset and offset times were estimated using the time at which the surface temperature reached the temperature of maximum density, 3.98°C, as a proxy.

Here, we present a description of a year-round temperature dataset from Lake Superior, which spans multiple locations and years. The measurements are of high temporal resolution and span the entire water column, presenting unique opportunities to investigate the thermal structure of the lake and the mechanisms that influence it. The year-round nature of the dataset offers a depiction of the lake during seasons where very little data has been available, including through periods of ice cover. In addition, Lake Superior is composed of somewhat distinct eastern and western basins, and having data

from multiple geographic locations during the study period provides insight into spatial variability throughout the lake.

The strength of this dataset lies not in revealing long-term trends, as this is not possible in the context of an eight year dataset. Instead, the record is useful in elucidating interannual variability in the thermal structure of the lake. Where previous studies have relied on surface temperatures to estimate the annual periods during which the lake is completely mixed, the distribution of this data vertically throughout the water column allows us to precisely characterize the times during the study period at which the water column is isothermal. The ability to observe the behavior of the entire water column in the moments leading up to and following stratification and overturn is fundamental in understanding the mechanisms driving these events, and the implications of their timing.

Austin and Colman (2007) found that rising lake surface temperatures are correlated with declining ice cover, and postulated that years of lower ice cover ultimately result in an earlier and longer summer stratified season. However, their conclusion was empirical, as opposed to mechanistic. Heat flux is, in part, a function of the temperature difference at the air-water interface. As such, over the spring warming period, it is reasonable to expect that the lake temperature would have a tendency to mitigate abnormally warm or cold initial temperatures through decreased or increased heat flux, respectively. This would mitigate the effect that winter conditions, including ice cover and its effects on heat content, have on the following summer. With several years of year-round data, we are able to characterize the extent to which variability in

winter conditions, as articulated in the lake's thermal structure, is "lost" during the spring warming season.

Further, the influence of ice cover on lake-atmosphere interactions is not easy to account for through one-dimensional modeling. It is reasonable to expect a negative correlation between heat content and ice cover (years with lower heat content experience more extensive ice cover). While such a scenario is likely the norm, the meteorological conditions preceding ice cover could have implications on the lake's thermal structure, whereby the lake does not always behave in this manner. For example, it is feasible that there could be a year in which a relatively thin surface layer of the lake is unusually cold, while the remainder of the water column is abnormally warm, resulting in both high ice cover and high heat content.

The mechanisms driving these phenomena and relationship between ice cover and heat content are not well understood. Ice imposes a barrier between the lake and the atmosphere, which must inhibit heat flux to some extent, but the dynamics of such an interaction are not well-characterized. For reasons discussed earlier, there is very little available data that documents the thermal structure of large lakes during periods of ice cover. The dataset discussed herein addresses this deficiency and sheds light on the thermal behavior of a partially ice-covered lake.

# 2.0 Background

## 2.1 Lake Superior

Lake Superior is located along the United States/Canada border, with shoreline in three U.S. states (Michigan, Minnesota, and Wisconsin), and one Canadian province (Ontario). It is part of the Laurentian Great Lakes System, along with Lake Michigan, Lake Huron, Lake Erie, and Lake Ontario, which ultimately flow into to the Atlantic Ocean through the St. Lawrence Seaway. Lake Superior is the largest of these lakes, in terms of surface area, volume, and both average and maximum depth.

Worldwide, Lake Superior is the largest freshwater lake by surface area, at approximately 82,100 $km^2$. It is the third largest freshwater lake by volume, containing approximately 12,000 $km^3$, or about 10%, of the world's freshwater. It is about 560 km long (from east to west) and about 260 km wide (from north to south), spanning about 2.5 degrees of latitude and about 7.5 degrees of longitude. The average depth of Lake Superior is approximately 150 m, and the maximum depth is 406 m.

Hydrologically, Lake Superior is the most inland of the Laurentian Great Lakes from the Atlantic Ocean. Lake Superior drains into Lake Huron through the St. Marys River, located at the southeastern end of the lake. It has more than 200 river inflows, and a residence time of approximately 200 years. Lake Superior can be divided into two sub-basins – the deeper eastern basin and the shallower western basin (see Figure 1). These are separated by a relatively shallow ridge extending northeast off of the Keweenaw Peninsula.

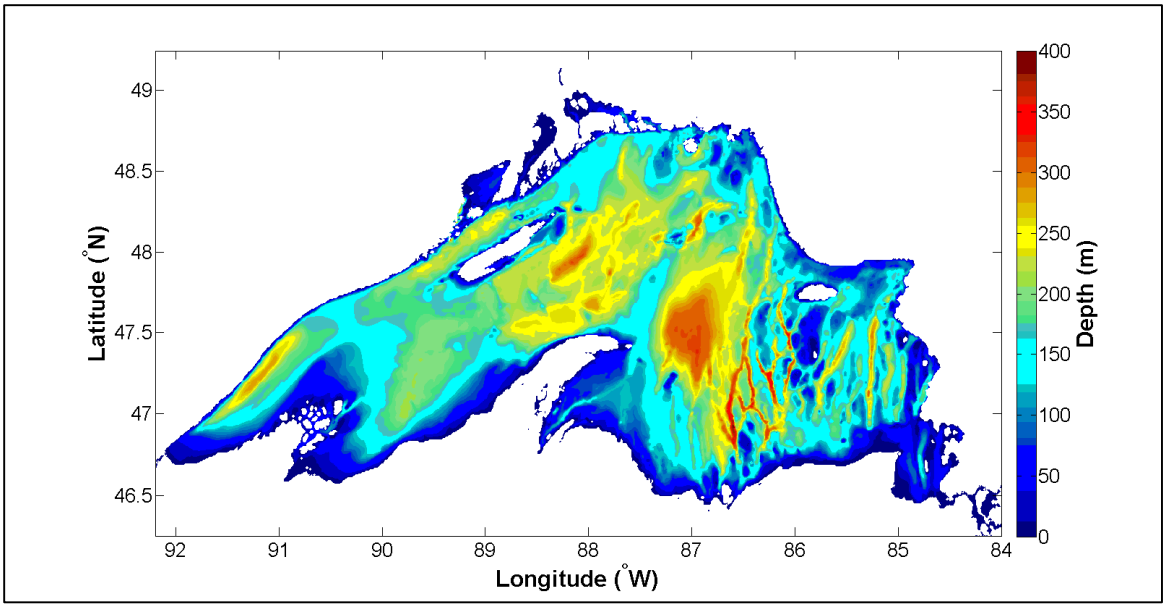


**Figure 1. Lake Superior Bathymetry.** Lake Superior has a maximum depth of 406m. It can be divided into two sub-basins – the deeper eastern basin, and the shallower western basin. These are divided by a relatively shallow ridge extending from the Keweenaw Peninsula (NOAA NGDC).

With its mid-latitude geographic position, Lake Superior experiences a strong annual meteorological cycle, with warm summers and cold winters. This translates into a strong annual signal in the lake's temperature and thermal structure. The lake positively stratifies in the summer, negatively stratifies in the winter, and turns over each fall and spring. Lake Superior receives ice cover during the winter, but does not ice-over completely every year.

## 2.2 Lake Stratification

Freshwater lakes stratify due to water's unique temperature-density relationship, in which the temperature of maximum density of water ($T_{MD}$) is 3.98°C at zero gauge pressure (P=0) (Figure 2). $T_{MD}$ decreases as pressure increases, so $T_{MD}$ is lower at greater depths in the water column. When surface heat fluxes cause the surface of the lake to either warm or cool away from $T_{MD}$, that water becomes less dense and, in the

absence of any disturbance, will float above the denser water below. The bottom of the water column, on the other hand, will be nearest to $T_{MD}$ throughout the year. As these processes progress, the water column can become separated into two distinct layers – the surface mixed layer, known as the epilimnion, and the bottom layer, known as the hypolimnion. In between these layers is a transitional layer, known as the thermocline, or metalimnion, which is observed as a pronounced temperature/density gradient. A greater density difference between the surface and bottom layers will, in general, lead to a steeper density gradient and, thus, a more stable thermocline.

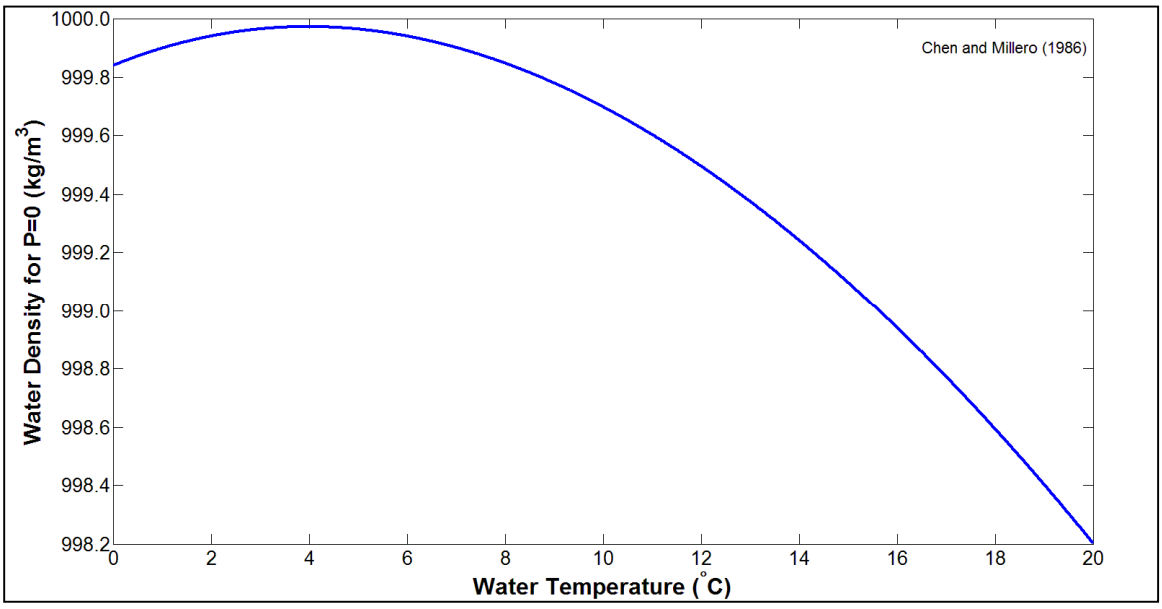


**Figure 2. Water Temperature-Density Relationship (Chen and Millero, 1986).**Water has a unique temperature-density relationship, in which its temperature of maximum density occurs at 3.98°C when P=0.

Wind is the primary kinetic energy input driving lake mixing, and can influence how stratification progresses. Stronger winds are able to mix a greater depth of the water column. In addition to the magnitude of the wind stress, the thermal structure of the water column is a contributing factor in determining to what depth a given wind will mix the water column. For example, when a lake is in a period of strong stratification, a

stable thermocline will be present, and a given wind event may only mix the lake as deep as the thermocline or may deepen the thermocline. In either case, distinct surface and bottom layers remain intact. However, when the temperature difference between the surface and bottom layers is small, and the thermocline is less stable, the same wind event may have enough energy to mix the entire water column.

This relationship between the stability of the water column and wind-driven mixing is responsible for the annual mixing patterns of the lake. Each time surface water in a lake warms or cools across the $T_{MD}$ threshold, the water column will mix. Lake Superior, which experiences cold winters and warm summers, mixes twice annually – once when surface water warms across $T_{MD}$ in the spring, and once when cooling across $T_{MD}$ in the fall. This pattern of twice-annual mixing is referred to as a dimictic mixing pattern (Lewis, 1983). Lake Superior, however, is unusual among dimictic lakes, because it does not become completely ice-covered in the winter every year.

Lake stratification has significance to both chemical and biological processes. When a lake is stratified, the bottom layer of the lake becomes sequestered from both the upper layer of the lake and the atmosphere. Oxygen and other gases diffusing into the lake from the atmosphere are distributed only though the surface mixed layer of the lake. When organisms residing in the bottom layer respire and consume oxygen, there is no mechanism for replenishing it. Therefore, lakes with high biological productivity and prolonged periods of stratification can experience periods of anoxia in the bottom layer of the lake, between mixing events.

Stratification can also influence photosynthesis. Nutrients have a tendency to sink to the bottom of the water column, in the form of decaying organic matter. These nutrients, along with sunlight, are the primary ingredients for photosynthesis. When these nutrients become sequestered at the bottom of the lake, photosynthesis is inhibited, because sufficient sunlight is present only near the surface of the lake. In such cases, since nutrients are only replenished during mixing events, prolonged stratification can lead to reduced photosynthesis.

In each of these cases, the length of the stratified season is important. Although the occurrence of anoxia or decreased photosynthesis also depends on such factors as the lake's productivity, morphology, and climate, the longer that surface and bottom layers are chemically isolated from one another, the more significant any oxygen or nutrient sequestration becomes. These issues are not currently issues within Lake Superior, but are relevant in other large lakes. As the Earth's climate is warming, it is likely that lakes will experience earlier and longer periods of summer stratification, increasing the extent and frequency of these events of anoxia and nutrient limitation. Therefore, it is important to understand the mechanisms that determine the timing of lake stratification. Such knowledge will be fundamental toward understanding what drives interannual variations in the timing of lake stratification, and how this timing may shift in the presence of climate change.

## 2.3 Heat Flux

A lake's thermal dynamics are ultimately driven by heat flux between the lake and its surrounding atmosphere. This heat flux can be separated into four distinct

components – net shortwave radiation, net longwave radiation, latent heat flux, and sensible heat flux. That latter three of these heat flux components are functions of the air-water temperature difference at the lake surface. They therefore act as equilibrative fluxes, because they drive the lake surface temperature toward the temperature of the overlying atmosphere. Shortwave radiation, on the other hand, is a unidirectional process that always results in a positive flux of heat energy into the lake, and is independent of the lake temperature or atmospheric temperature.

The total heat flux into the lake is simply the sum of the four heat flux terms, which are described in the following sections:

$$Q = Q_{SW} + Q_{LW} + Q_{SEN} + Q_{LAT} \qquad \text{(Equation 1)}$$

### 2.3.1 Shortwave Radiation

Shortwave heat flux ($Q_{SW}$) is a function of the intensity of incoming solar radiation. As such, the magnitude of shortwave heat flux depends on latitudinal position, and follows an annual cycle. The overall clear-sky distribution of shortwave radiation can be determined for any location on Earth. However, fluctuations in shortwave radiation do still occur on regional scales, as sunlight passing through the atmosphere is absorbed or reflected. Cloud cover absorbs up to 80% of incoming solar radiation, which can result in significant fluctuations in the amount of shortwave radiation reaching the lake surface. Once this radiation reaches the lake surface, the amount absorbed into the lake depends on the albedo of the water surface. Under open-water conditions, only

about 7% of shortwave radiation is reflected away from the lake (Payne 1972), allowing over 90% to be absorbed by the lake as heat energy. Under ice cover, however, 40-80% of shortwave radiation is reflected, depending on the age of the ice, drastically reducing the amount of heat energy absorbed by the lake.

### 2.3.2 Longwave Radiation

All matter emits energy to its surroundings in the form of longwave radiation. In the context of a lake, the lake emits longwave radiation into the atmosphere while the atmosphere simultaneously emits longwave radiation into the lake. This upwelling and downwelling radiation results in a net heat flux between the air and the atmosphere, which can be estimated as follows:

$$Q_{LW} = \varepsilon\sigma\left(T_A{}^4 - T_W{}^4\right) \qquad \text{(Equation 2)}$$

Where:

- $Q_{LW}$ is the net longwave radiation ($W \cdot m^{-2}$)
- $\varepsilon$ is the emissivity of the lake surface (approximately 0.98)
- $\sigma$ is the Stefan-Boltzman constant ($5.67 \times 10^{-8}$ $W \cdot m^{-2} \cdot K^{-1}$)
- $T_A$ and $T_W$ are the air and water temperatures, respectively (in K)

### 2.3.3 Sensible Heat Flux

Sensible heat flux is a form of turbulent heat flux, meaning it is facilitated by a velocity difference at the air-water interface. Eddies arise from this velocity difference, and transport heat energy between the lake surface and the overlying atmospheric boundary layer, referred to as sensible heat flux. Sensible heat flux can be modeled with the following expression:

$$Q_{SEN} = \rho_A c_p C_H (T_A - T_w)|u_A - u_W| \quad \text{(Equation 3)}$$

Where:

- $Q_{SEN}$ is the net sensible heat flux ($W \cdot m^{-2}$)
- $\rho_A$ is the density of air (in $kg \cdot m^{-3}$)
- $c_p$ is the heat capacity of water (4180 $J \cdot kg^{-1} \cdot K^{-1}$)
- $C_H$ is a unitless scaling coefficient ($3 \times 10^{-4}$)
- $T_A$ and $T_W$ are the air and water temperatures, respectively (in K)
- $u_A$ and $u_W$ are the velocities of the air and water, respectively (in $m \cdot s^{-1}$)

### 2.3.4 Latent Heat Flux

Latent heat flux is another form of turbulent heat flux. It accounts for the energy required for water to change phase. Evaporation results in a negative heat flux, while condensation results in a positive heat flux. The net heat flux resulting from these processes can be modeled as follows:

$$Q_{LAT} = \rho_A L C_E (q_z - q_0)|u_A - u_W| \quad \text{(Equation 4)}$$

Where:

- $Q_{LAT}$ is the net sensible heat flux ($W \cdot m^{-2}$)
- $\rho_A$ Is the density of air (in $kg \cdot m^{-3}$)
- L is the latent heat of water (2,260,000 $J \cdot kg^{-1}$)
- $C_E$ is a stability-dependent transfer coefficient
- $q_z$ is the specific humidity at a given height above the water
- $q_0$ is the specific humidity at the water surface
- $u_A$ and $u_W$ are the velocities of the air and water respectively (in $m \cdot s^{-1}$)

# 3.0 Methods

## 3.1 Mooring Arrays

The Lake Superior mooring array has consisted of one or more moorings deployed continuously since 2005 (Table 1 /Figure 3/Figure 4). The Western Mooring (WM), first deployed in 2005, along with the Eastern (EM) and Central (CM) Moorings, each first deployed in 2008, form the "core mooring" array that is still presently in service. Beginning in fall 2008, this core mooring array was supplemented by a combination of one or more "outer moorings" – the Far Western (FWM), Northern (NM), Southern (SM), and Far Eastern Moorings (FEM).

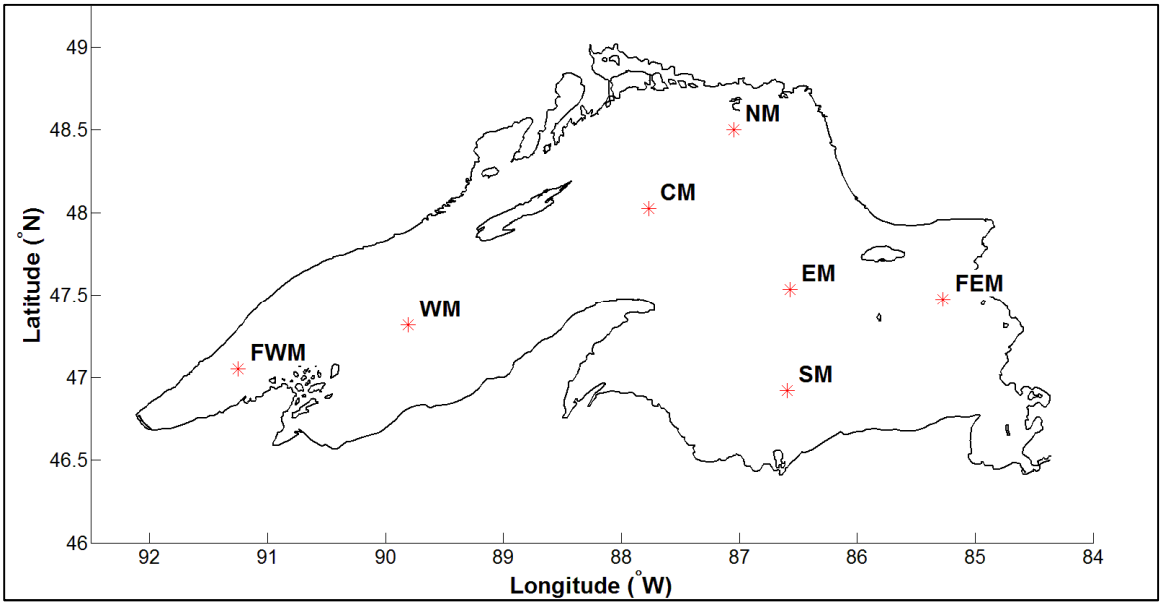


**Figure 3. Mooring Location Map.** The locations of all seven Lake Superior moorings are shown.

| | Mooring Name | Latitude (N) | Longitude (W) | Water Column Depth (m) |
|---|---|---|---|---|
| Core Moorings | Western Mooring (WM) | 47° 19.018' | 89° 48.520' | 185 |
| | Central Mooring (CM) | 48° 1.384' | 87° 46.006' | 255 |
| | Eastern Mooring (EM) | 47° 32.186' | 86° 34.261' | 213 |
| Outer Moorings | Far Western Mooring (FWM) | 47° 3.005' | 91° 14.928' | 170 |
| | Northern Mooring (NM) | 48° 29.972' | 87° 2.935' | 201 |
| | Southern Mooring (SM) | 46° 55.252' | 86° 35.805' | 384 |
| | Far Eastern Mooring (FEM) | 47° 28.375' | 85° 16.394' | 247 |

**Table 1. Mooring Locations.** This table provides the latitude, longitude, and water column depth for each mooring.

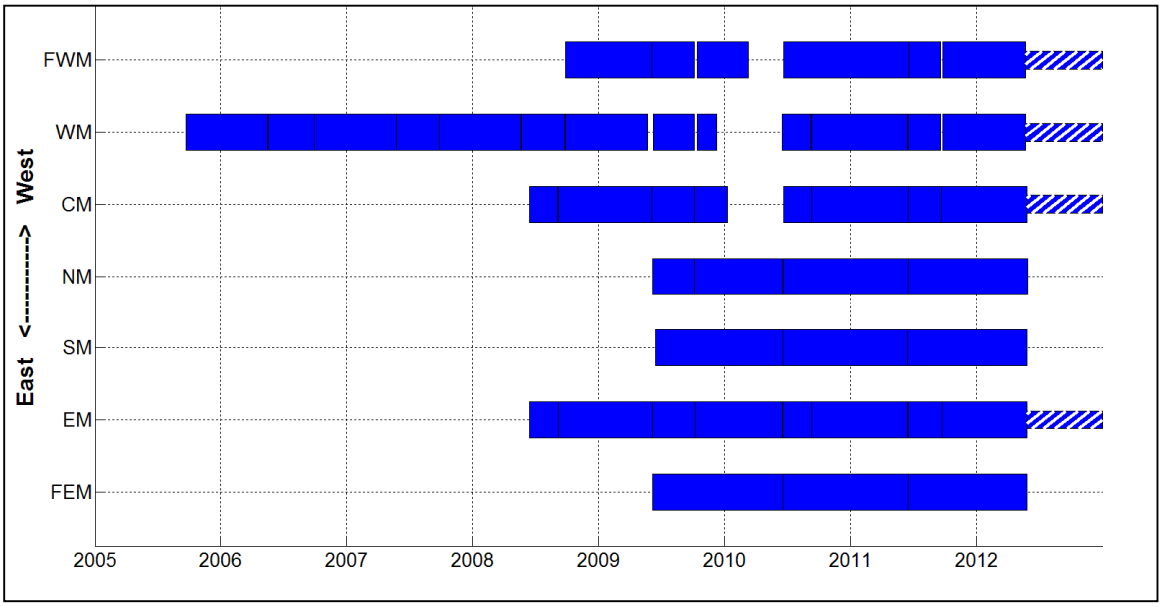


**Figure 4. Mooring Deployment History.** The deployment history of the three core moorings (WM, CM, EM) and four outer moorings (FWM, NM, SM, FEM) is shown from 2005-2012. There is a lapse in data over the 2009/2010 winter at three moorings, due to faulty cables. The core mooring array was re-deployed, as well as the Far Western Mooring; all other moorings have been removed from service.

Each mooring is equipped with 10 to 13 thermistors, which are distributed throughout the water column (Figure 5). Thermistors are spaced more closely near the surface, where the spatial scales of temperature variability are smallest, and they are spaced father apart in the bottom portions of the lake, where the water temperature remains relatively constant throughout the year. Moorings do not extend to the water surface. Instead, the uppermost thermistor on each mooring is located at a depth of 7 to

10 meters below the water surface. The bottommost thermistor is located approximately 3 to 5 meters above the lake bottom, with the mooring anchor and acoustic release positioned below.

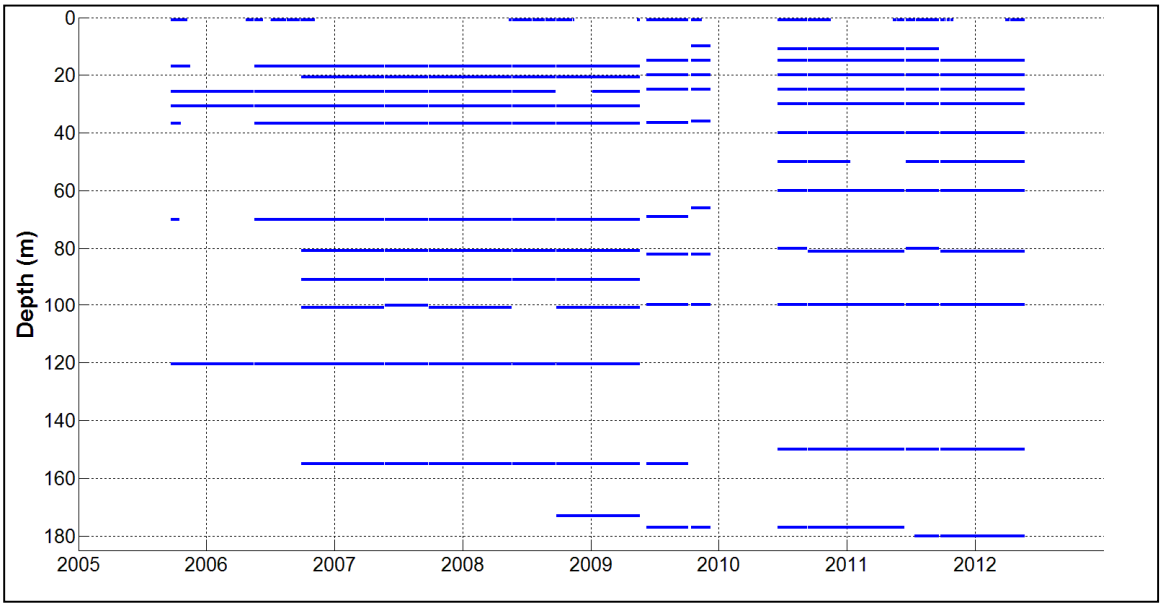


**Figure 5. Western Mooring Thermistor Depth Coverage.** The presence of active thermistors is shown by lines. Thermistors are spaced more closely near the surface, where temperature varies more substantially over smaller changes in depth.

The placement of the core mooring array was chosen to coincide with the locations of the National Data Buoy Center (NDBC) buoys, with the Western, Central, and Eastern Moorings deployed within 1 to 2 km of NDBC buoys 45006, 45001, and 45004, respectively. These NDBC buoys record near-surface (1-m depth) temperature readings, which can be used to fill-in surface temperatures for the core mooring deployment over the summer ice-free season, when the NDBC buoys are in service. The emphasis of this dataset, however, is on winter thermal structure. In the winter, there is very little temperature variability near the surface, so the uppermost thermistor provides a reasonable estimate for the surface temperature of the lake at all mooring locations.

A variety of thermistor models have been used throughout the deployments, including Brancker Research (RBR) TR-1000, TR-1050, TR-1060, and TD-2050 sensors, and Seabird Electronics SBE-39 and SBE-39P sensors. The TD-2050 and SBE-39P models contain pressure sensors in addition to temperature sensors, which are used to verify that thermistors are deployed at the designed depth. Every mooring is equipped with at least one of these pressure sensors. Measurement frequencies are dictated by the storage capacity of the instruments, with the TR-1000 and SBE sensors taking measurements every 10 minutes, and the TR-1050, TR-1060, and TD-2050 sensors taking measurements every 1 minute. All temperature data considered in this paper has been averaged over hour intervals. This reduces noise in the data and establishes a uniform time scale amongst moorings and thermistors.

Once deployed, moorings remain in continuous operation, being briefly removed only once or twice a year to retrieve data and replace batteries. In fall 2009, a faulty batch of mooring wire was used, causing the Far Western, Western, and Central moorings to collapse during that deployment period, when the wire corroded. As a consequence, there is a gap in temperature data at these moorings from Winter 2009 through their Spring 2010 re-deployment. This represents the only significant gap in thermistor data over the mooring array's deployment history. Additionally, there is not NDBC buoy data at the Western Mooring location in 2007, so summer surface temperature estimates are not available at the Western Mooring for that year.

The Western and Eastern Moorings are also equipped with Acoustic Doppler Current Profilers (ADCPs), and those and other moorings have been periodically

equipped with additional instrumentation, including ADCPs, ice profilers, $O_2$ sensors, $NO_3$ sensors, and sediment traps. Only thermistor data is presented and discussed in this paper; however, ADCP data has recently been used to examine near-inertial oscillations within the lake, and is discussed in detail in Austin (2013).

## 3.2 Ice Data

Lake Superior ice cover time-series were extracted from Interactive Multisensor Snow and Ice Mapping System (IMS) data, available through the National Environmental Satellite, Data, and Information Service (NESDIS), which is part of the National Oceanic and Atmospheric Administration (NOAA). The IMS data is derived from satellite imagery, and distributed as daily snow and ice cover maps for the northern hemisphere in both 4-km and 24-km grid formats. For each grid point on these maps, there is a corresponding value that describes whether the surface at that grid location is open land, open water, snow, or sea ice. The data are intended to depict the presence or absence of snow and ice, with no information regarding snow or ice thickness or density. These IMS snow and ice data are freely available (NOAA/NESDIS 2004), with 24-km data spanning February 1997 to present, and 4-km data spanning February 2004 to present.

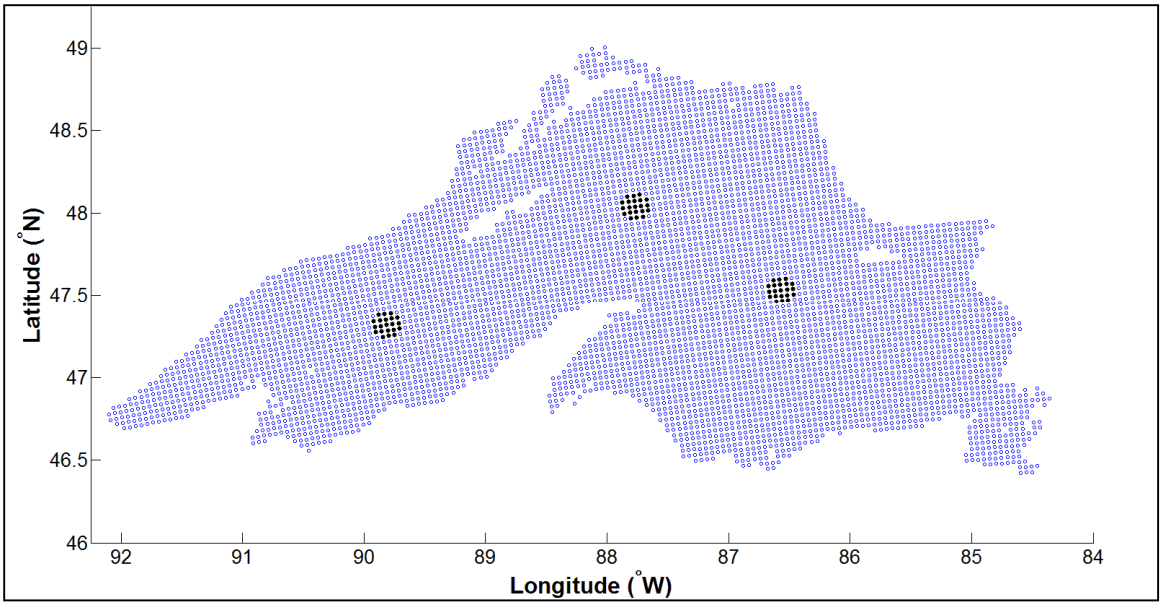


**Figure 6. Lake Superior Ice Data Grid.** Lakewide ice data was extracted from the NOAA/NESDIS IMS northern hemisphere grid with 4-km spatial resolution. Local ice cover datasets were extracted using a 10-km radius around mooring locations.

The 4-km IMS snow and ice grid was used to assemble Lake Superior ice cover datasets. Lakewide ice cover was extracted using a 6042 grid-point mask over the lake (Figure 6). Further, 4-km is a sufficiently high resolution to analyze not only interannual variations in ice cover for the lake as a whole, but also the spatial variability within the lake during any given year. Specifically, the high spatial resolution of the data facilitates the extraction of a distinct local dataset for each mooring location. Rather than developing these local ice cover datasets using the single grid point on which each mooring falls, ice cover data was extracted from 10-km radius around each mooring. The 10-km radius is intended to reduce noise in the data, since the data is being averaged over 21 grid points surrounding the mooring, as opposed to just one. As a result, it provides information as to the fraction of the area surrounding the mooring that is covered by ice, as opposed to a simple present/absent value. A 10-km radius was chosen in order to incorporate a meaningful number or grid points surrounding each mooring. Varying this

radius does not significantly alter local ice cover time-series and, thus, results based on ice data are not sensitive to this value.

To put this recent data in context, historical ice cover data was obtained from Great Lakes Ice Atlas, which is a compilation of ice cover data from various data sources for the Great Lakes beginning in 1973 (Assel 2003; Assel 2005; Wang et al. 2012). Using this data, winter average ice cover (December through May) was calculated for Lake Superior over this historical period in order to understand how current ice cover conditions on the lake compare to conditions experienced by the lake over the previous few decades.

# 4.0 Results

## 4.1 Dimictic Mixing Pattern

The Lake Superior thermistor record shows a dimictic temperature pattern, with a period of strong positive stratification each summer, and periods of weaker negative stratification each winter (Figure 7). Between these periods of stratification, the lake experiences a transition period, during which it is effectively isothermal during both spring warming and fall cooling.

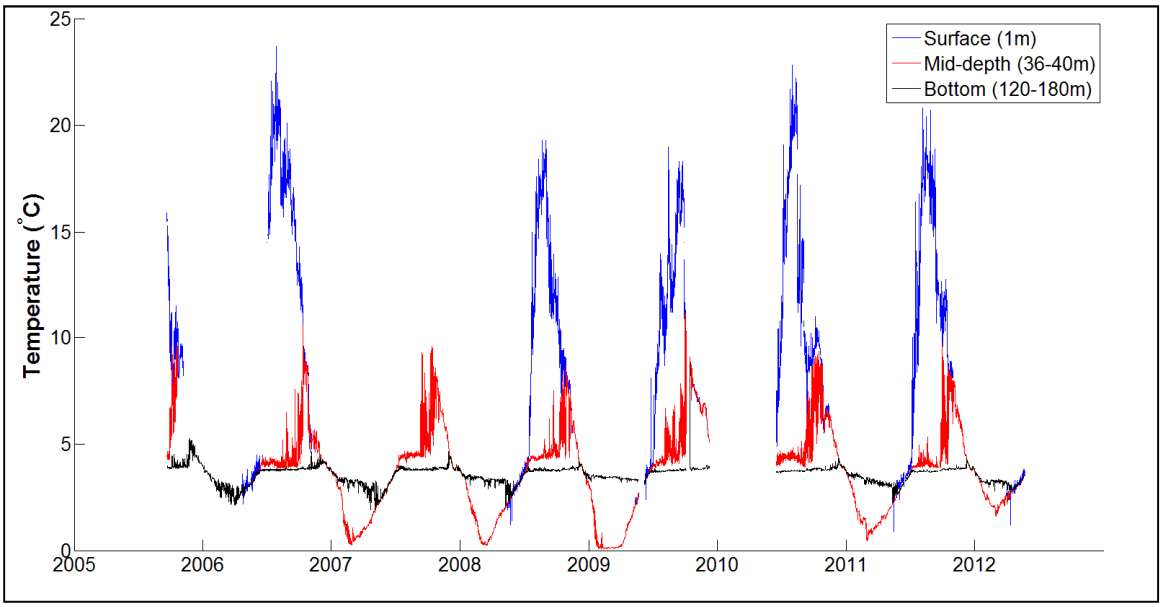


**Figure 7. Western Mooring Thermistor Data.** The Western Mooring time-series is shown as an example of the data collected from the mooring array. In this figure, a surface thermistor (1m depth), a mid-depth thermistor (36-40m depth), and a bottom thermistor (120-180m depth) are plotted for the duration of the Western Mooring's deployment history. The range in depths for the middle and bottom thermistors is due to thermistors being deployed at varying depths throughout the moorings history (see Figure 5). Note that in 2007, there was no available NDBC surface temperature data at this location; this was not necessarily a colder year. The mooring collapsed in 2010, due to faulty mooring cable, representing the only significant gap in thermistor data.

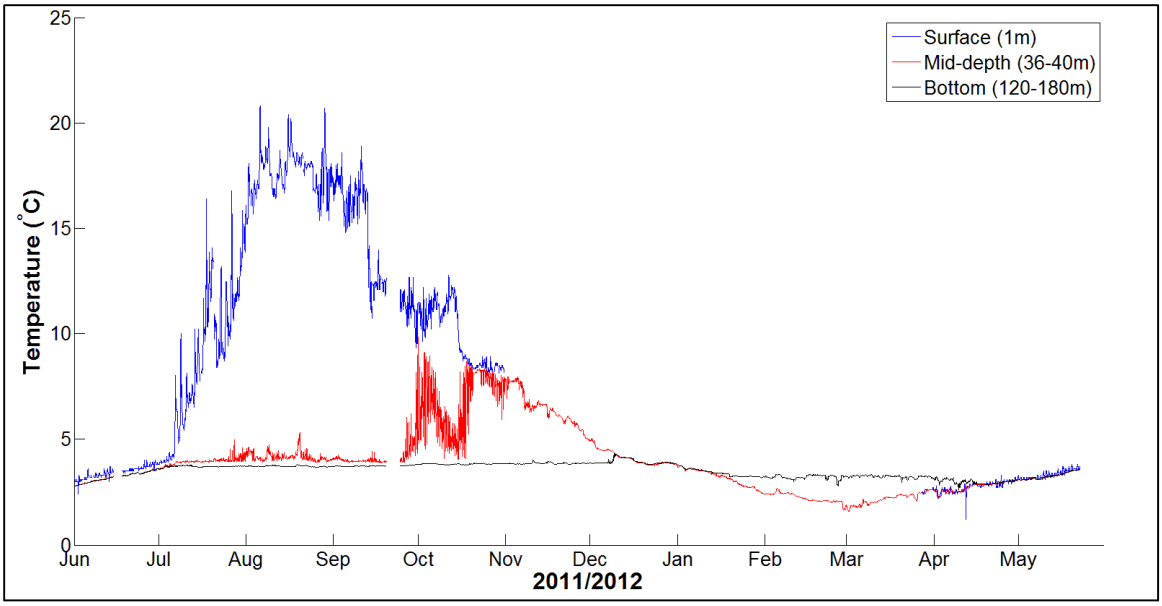


**Figure 8. Western Mooring Dimictic Annual Cycle.** One year of temperature data at the Western Mooring is focused on, to demonstrate the dimictic annual mixing cycle of Lake Superior. In this figure, a surface thermistor (1m depth), a mid-depth thermistor (36-40m depth), and a bottom thermistor (120-180m depth) are plotted for spring of 2011 through spring of 2012.

Beginning in the spring, after the collapse of any winter stratification, Lake Superior has a water column that is isothermal and below $T_{MD}$. As such, during this warming period, positive heat flux at the surface of the lake is distributed throughout the entire water column. This continues until the water column reaches a water temperature near $T_{MD}$. As discussed in Section 2.2, at temperatures above this $T_{MD}$ threshold, positive surface heat flux results in surface water that is less dense than the water below, and the lake begins to stratify. Once this stratified layer is established, incoming heat energy is only distributed throughout the surface layer. Throughout the summer, temperatures in the surface mixed layer continue to increase, with surface temperatures approaching or exceeding 20°C. Temperatures in the lower portion of the lake remain roughly constant throughout the summer, near $T_{MD}$.

Heat flux becomes negative at the end of the summer season, and heat energy begins to be lost from the surface mixed layer, causing it to cool. As the temperature of the surface mixed layer decreases, the density gradient across the thermocline becomes less pronounced, and the stratification of the water column becomes correspondingly less stable. This less-stable stratification renders the water column more susceptible to wind-driven mixing. Wind events begin to deepen the thermocline, resulting in a deeper and cooler surface mixed layer. Once the temperature of the surface mixed layer reaches a temperature near $T_{MD}$, the water column again completely mixes, and cools isothermally until negative stratification forms.

Negative stratification is observed every winter, to varying degrees, with water temperatures in the lower portion of the lake remaining between 3-4°C for the duration of the winter, and temperatures near the surface reaching minimum temperatures less than 1°C most years. As winter ends and heat flux becomes positive, incoming heat energy is again distributed through the upper portion of the negatively stratified water column. Once the surface mixed layer reaches a temperature of around $T_{MD}$, the water column mixes once again, and continues to warm throughout the spring. This dimictic cycle is observed every year in the Lake Superior mooring thermistor data, and at every mooring location.

## 4.2 Interannual Variability

Over the years comprising the study period, significant interannual variation is observed within the data. Thermistor data from the Western Mooring reveals that of the years it has been deployed, there was relatively strong stratification in the summers of

2006 and 2010. Above average temperatures are also observed in the upper water column at the Central and Eastern Moorings in 2010 (they were not yet deployed in 2006), suggesting this was a lakewide trend. None of the study years stand out as having anomalously cold summer surface water temperatures.

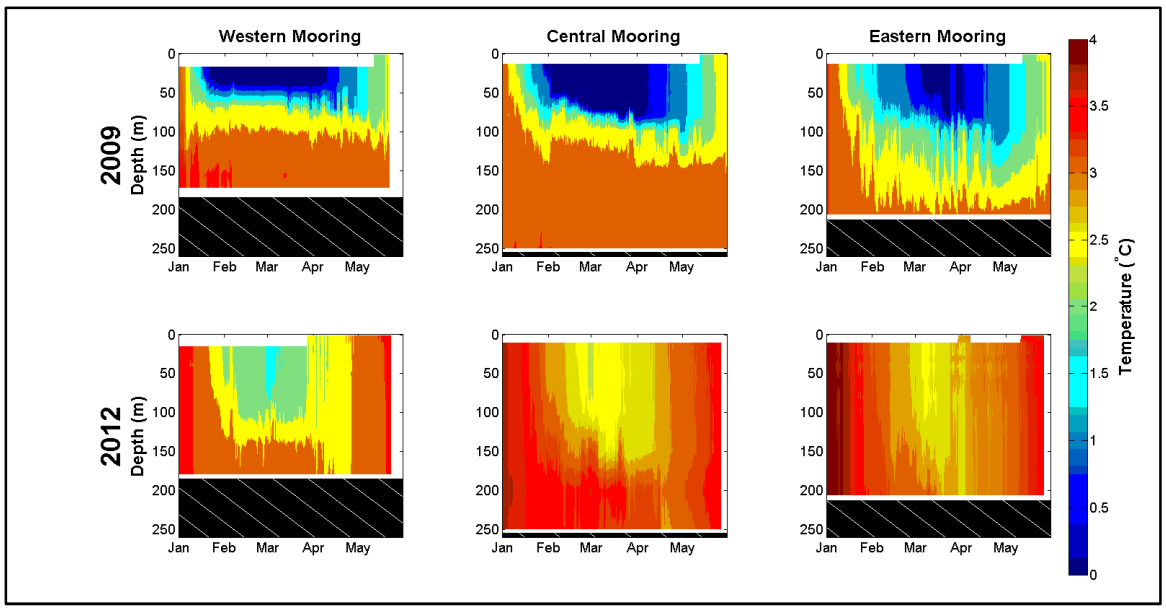


**Figure 9. Winter Spatial and Interannual Variability.** Winter thermal structure is shown for the three core moorings from both the cold winter of 2008/2009 and the warm winter of 2011/2012.

Even more dramatic is the interannual variability in winter heat thermal structure (Figure 9). Throughout the study period, unusually strong winter stratification is observed in the winter of 2009. This is particularly evident at the Western Mooring, where temperatures in the upper water column fall to near 0°C and remain there for the majority of the winter season, from late January through late March, while temperatures below that remain approximately 2.5-3.5°C. Temperatures near 0°C are also sustained in the upper water column at the Central Mooring throughout the winter of 2009; however, the duration of this relatively strong stratification is shorter at this mooring than at the Western Mooring, lasting from early February through late March. Below average

temperatures are also observed in the upper water column of the Eastern mooring. However, unlike the Western and Central moorings, upper water column temperatures at the Eastern Mooring only briefly approached 0°C, during early March. These near-zero temperatures indicate the possible presence of ice cover, which will be discussed further in Section 4.3.

This is in stark contrast to the thermal structure observed at the same moorings during the warmer winter of 2012. During the 2012 winter, the Eastern Mooring, in particular, barely stratified. A maximum temperature difference of less than 1°C across the water column was observed at the Eastern Mooring during that season. Likewise, the maximum temperature difference was less than 1.5°C at the Central Mooring, and less than 2°C at the Western Mooring. In 2009, all three moorings saw temperature differences across the water column of more than 3°C (Figure 9).

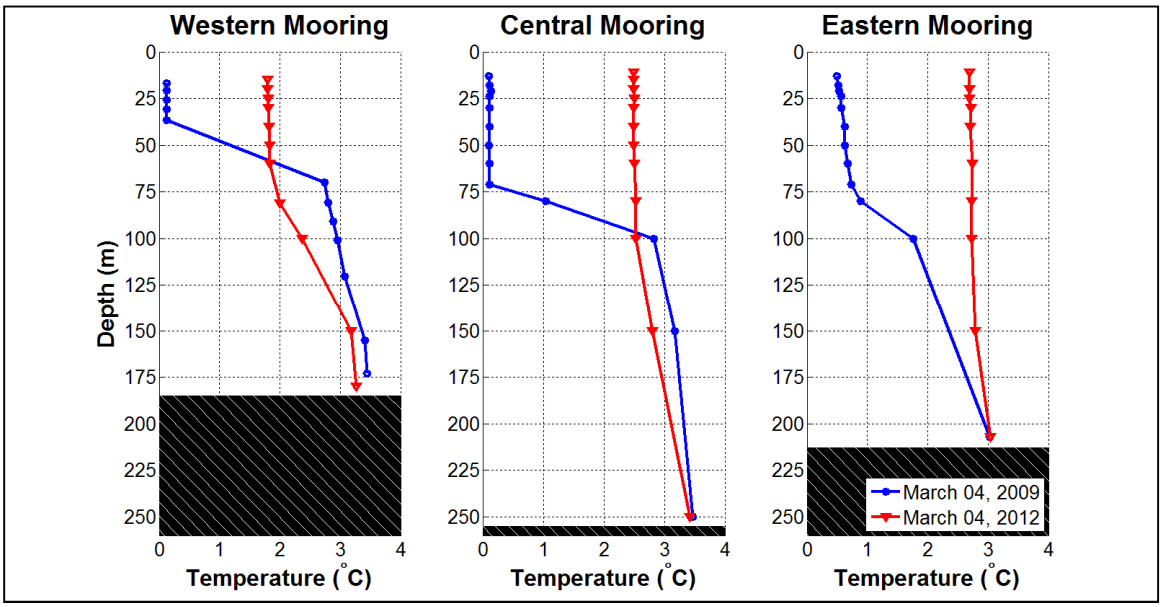


**Figure 10. Winter Thermal Structure Profiles.** Water column temperature profiles are shown from March 04, 2009 and March 04, 2012, a date near peak negative stratification each year.

In addition to substantially colder temperatures in the upper water column in 2009 than in 2012, the depth of the thermocline is much deeper in 2012 than in 2009 (Figure 10). At all three of the core mooring locations, a significantly deeper thermocline is observed in the ice-free winter of 2012. This variation is not trivial, with the thermoclines observed more than 50 meters deeper at all three moorings in 2012 than in 2009. As mentioned previously, stratification at the Eastern Mooring is extremely weak in the winter of 2012. At that location, the temperature profile was roughly isothermal for approximately the top 150 meters of the water column, with only the bottom 50 meters deviating slightly from that temperature. Thermoclines at the Western and Central Moorings are also much less steep in the winter of 2012 than the winter of 2009, but this difference is not as pronounced as at the Eastern Mooring.

There is very little interannual variability in hypolimnion temperatures during summer stratification, but there is some variability in hypolimnion temperatures during the winter. At the Western Mooring, for example, seasonal average temperatures at the bottom of the water column are consistently at 3.8 ± 0.1 °C during periods of summer stratification, consistent with $T_{MD}$ at that depth. However, during winter stratified periods, seasonally averaged hypolimnion temperatures ranged from 2.9 to 3.4 °C over the study years.

While this year-to-year variability is quite small, at only half of a degree, it is worth noting. The consistent summer hypolimnion temperatures suggest that a stable thermocline forms relatively rapidly once the temperature of the water column nears $T_{MD}$ each year, thereby preventing incoming heat energy from being mixed through the

bottom portions of the water column. This is in contrast to the winter, where the higher variability suggests that it takes longer for a stable density gradient to form, allowing the water column to remain vertically mixed and isothermal to temperatures below $T_{MD}$, while heat loss continues from throughout the entire water column. Further, a lower water column stability near the onset of winter stratification suggests that the water column may be more susceptible to wind-driven mixing at the onset of winter, and that the onset of winter stratification is more dependent upon calm periods of low wind than is the onset of summer stratification.

## 4.3 Ice Cover

Historical ice cover data useful for putting the ice coverage observed during the study period in a longer-term context. When examining ice cover data from Great Lakes Ice Atlas from 1973 through 2012 (Assel 2003; Assel 2005; Wang et al. 2012), it is clear that ice cover averages have been declining (Figure 11). There was, in general, much more ice cover in the 1970s and 1980s than there has been since the late 1990s. This is consistent with findings that the duration of ice cover is decreasing on lakes and rivers in the northern hemisphere (Magnuson 2000).

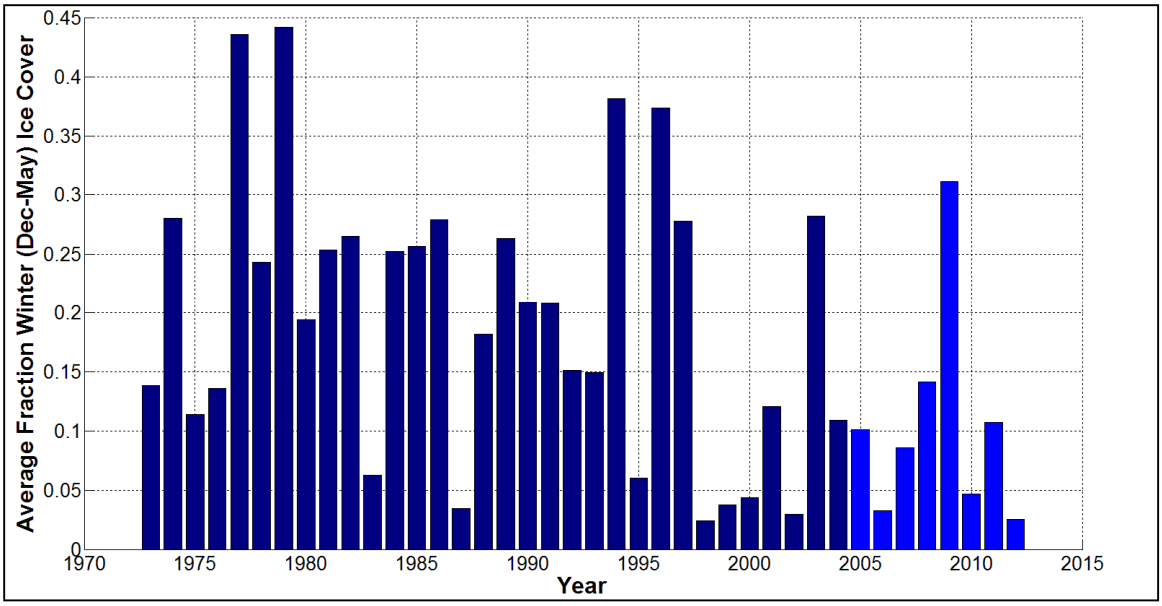


**Figure 11. Historical Lake Superior Ice Cover.** Historical data from the Great Lake Ice Atlas (1973-2004, darker) and the Ice Mapping System (2005-2012, lighter) show the average winter ice cover on Lake Superior for years 1973-2012.

When considering the study years (2005-2012), 2009 is the only year that stands out as having significant ice cover. 2009 experienced the highest average ice cover of any year since 1996, with ice cover comparable to levels typical of the 1970s and 1980s. The remainder of study years received low levels of ice cover, especially when considered in a long-term context. In particular, 2006, 2010, and 2012 received very little ice cover, with 2012 experiencing the lowest seasonally averaged ice cover on record. In these years of especially low ice cover, ice only forms within the bays and the perimeters of lake basins, and there is no substantial open-water ice cover.

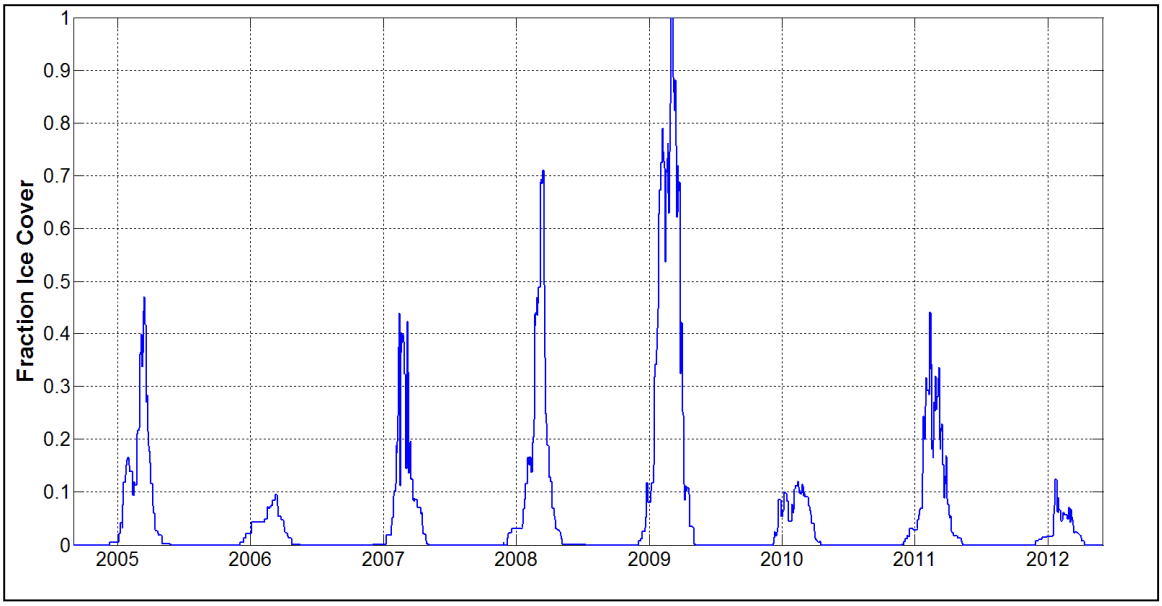


**Figure 12. Lake Superior Lakewide Ice Cover Time-series.** The fraction of lakewide ice cover is plotted for the years comprising the study period.

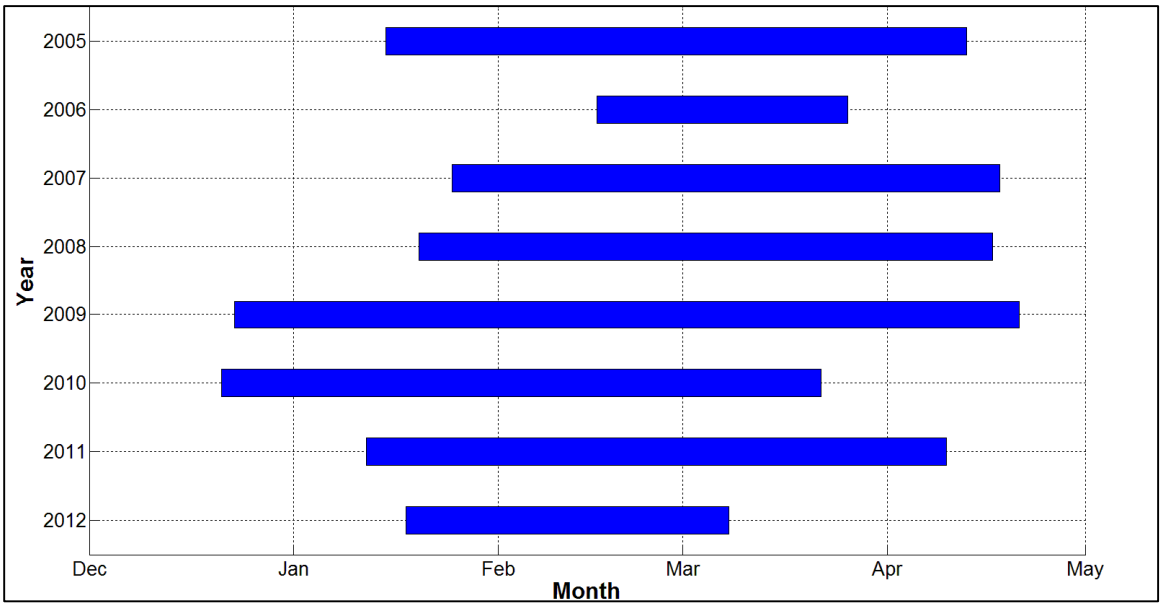


**Figure 13. Duration and Timing of Lake Superior Ice-Covered Season.** Ice-on and ice-off dates are shown for the years comprising the study period. Ice-on and ice-off dates were estimated using the first and last days, respectively, each year when the lake is at least 5% ice covered.

A daily lakewide ice cover time-series (Figure 12) reveals that 2009 was the only year during the study period in which the lake iced over completely, albeit briefly, from March 2 to March 6. With the exception of 2008, during which the ice received a

maximum ice cover of about 70%, ice cover peaked with less than 50% of the lake surface covered in ice in all other years during the study period. Using a metric of 5% lakewide ice cover to estimate ice-on and ice-off dates on the lake (Figure 13), ice-on occurred during study years as early as late December, and as late as mid February. Ice-off dates ranged from early March to late April. The duration of the ice-covered season is generally correlated with the extent of ice cover, with this correlation being more due to a correlation between ice extent and ice-off date than between ice extent and ice-on date. A metric of 5% ice cover is more useful in this discussion than 1%, for instance, because it is the point at which ice is generally first observed around the perimeter of major lake basins. Therefore, it is more representative of lakewide conditions, as opposed to conditions around localized bays and basins.

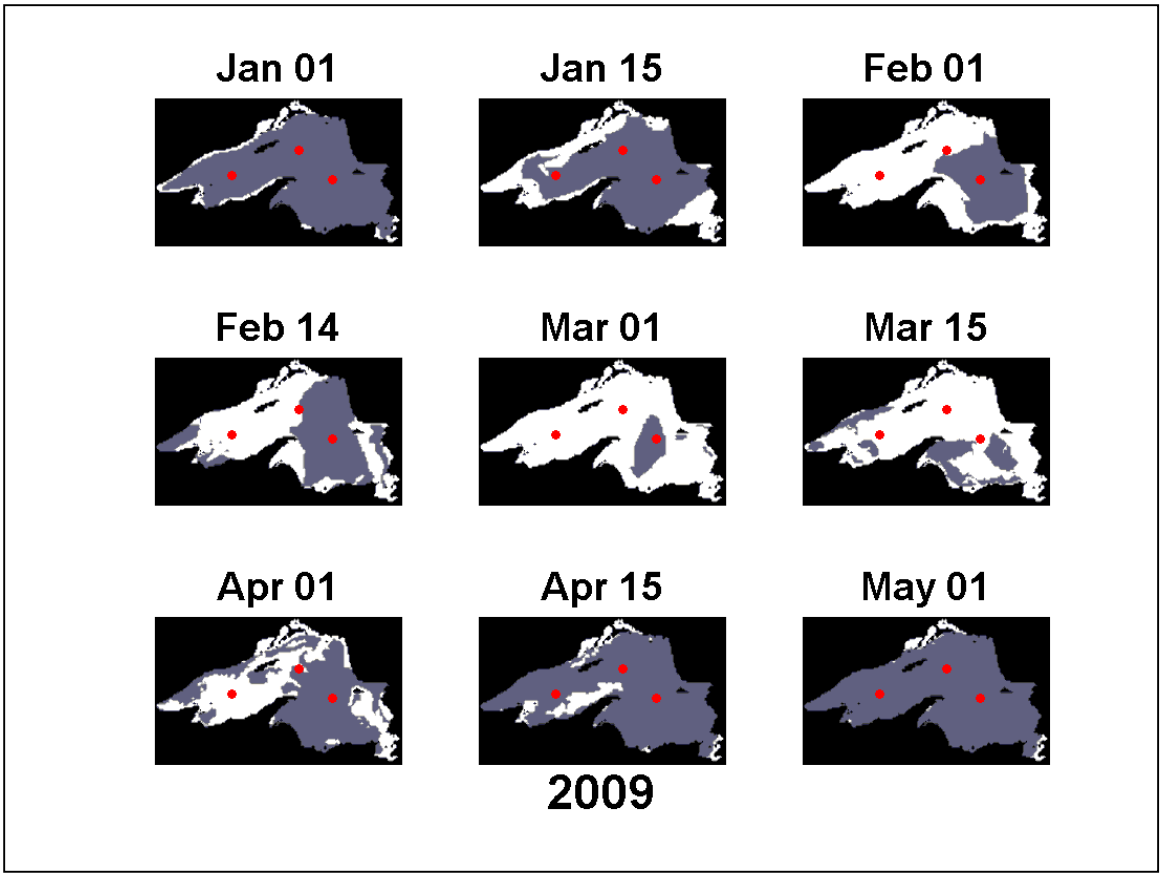


**Figure 14. 2009 Ice Cover Progression.** The progression of ice cover throughout the 2009 winter is shown. Ice is depicted as white and open water as gray. The Western, Central, and Eastern Moorings are shown as dots.

There is significant spatial variation throughout the lake, in terms of the timing and duration of ice formation (Figure 14). Ice formation generally follows a similar progression each year, with ice cover progressing further in high-ice years than lower-ice years. The first portions of the lake to freeze are generally the northern bays. Ice cover then proceeds to form around the southern perimeter of the lake. The western portions of this southern perimeter, around the Bayfield and Keweenaw Peninsulas, generally freeze earlier than the eastern portions, including Whitefish Bay. This ice cover then continues to extend further into the open-water portions of the lake. Of these open-water areas, the western basin of the lake freezes earlier than the eastern basin. The deep part of the eastern basin is the last portion of the lake to freeze. Ice-out patterns are more variable,

but ice in the eastern basin of the lake generally melts earlier than ice in the western basin.

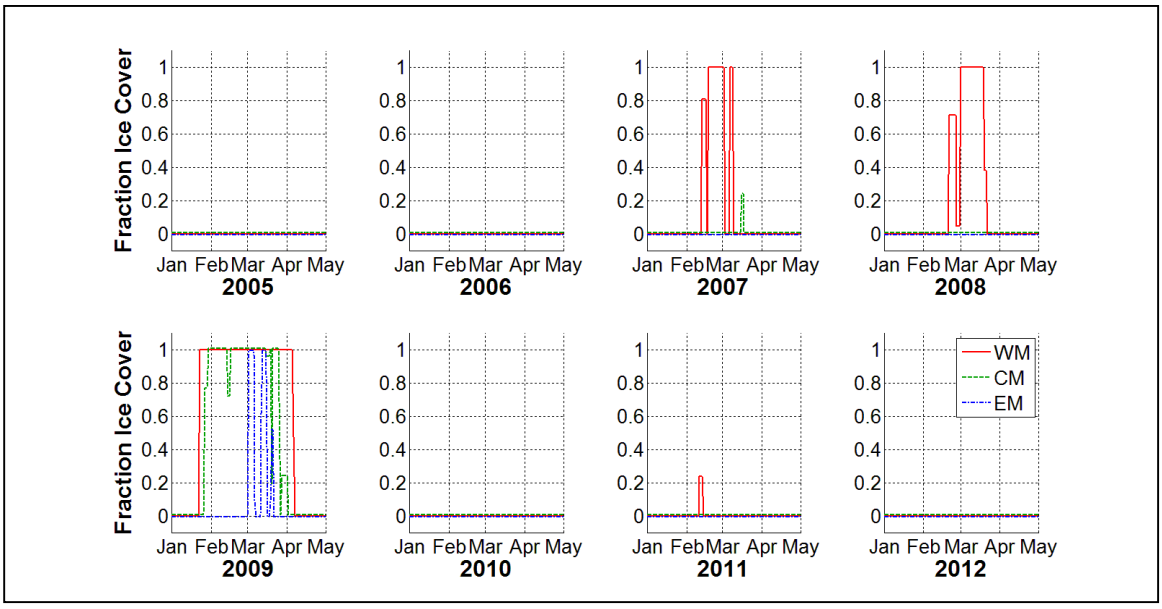


**Figure 15. Local Ice Cover around Moorings.** Local ice cover time-series are shown for the three core moorings for years comprising the study period.

Of the three core moorings, the Western Mooring experiences ice cover most often (Figure 15). During the study period, the Western Mooring location became ice covered in 2007, 2008, and 2009. With the exception of a small amount of ice cover in the vicinity of the Central Mooring in 2007, 2009 was the only year in which the region around the Central and Eastern Moorings iced over. The duration of this ice cover was shorter around the Central Mooring than at the Western Mooring, and was shorter yet around the Eastern Mooring. No moorings received local ice cover in 2005, 2006, 2010, or 2012, and only a minimal amount of ice was briefly present around the Western Mooring in 2011. Considering local ice cover around the core moorings during the study years, the Western Mooring, without exception, experienced the greatest amount of local ice cover, earliest ice formation, and longest ice duration each year. Meanwhile, the

Eastern mooring experienced the least amount of ice cover, latest ice formation, and shortest ice-covered seasons. This is consistent with the progression of ice formation discussed above, as the Western Mooring is located in the western basin of the lake, and the Eastern Mooring is located in the lake's eastern basin.

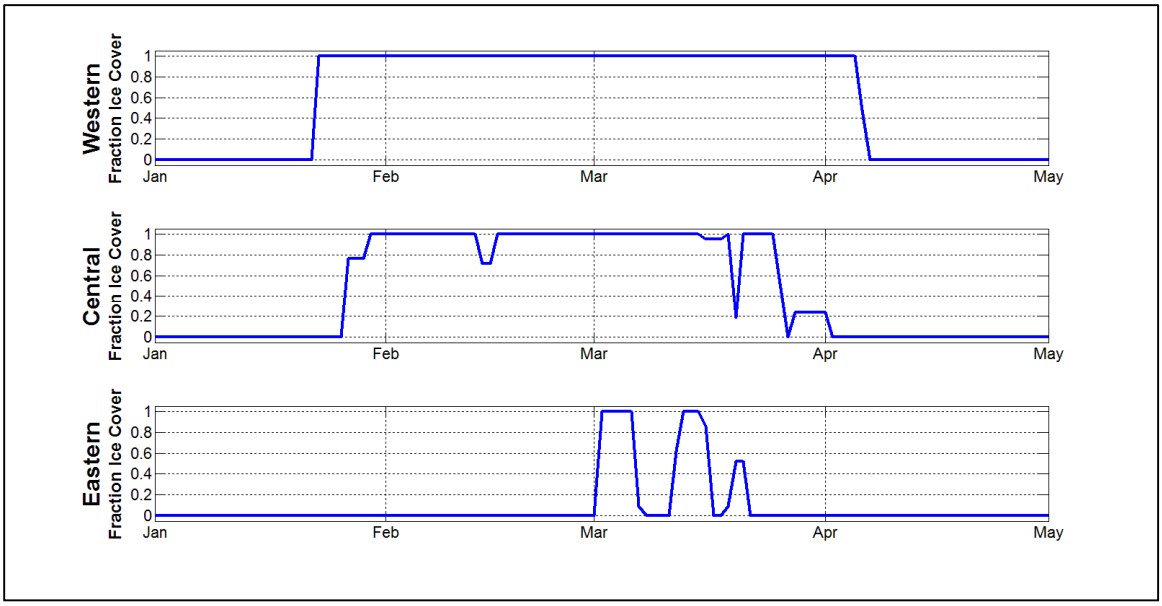


**Figure 16. Core Mooring Local Ice Cover, 2009.** Ice-cover time-series are presented for the Western, Central, and Eastern Moorings for the winter of 2009.

Focusing on 2009, as it is the only year with substantial lakewide ice cover, local ice cover time-series are consistent with the plots shown in Figure 14. The Western Mooring is the first of the core moorings to ice over, and the Eastern Mooring is the last. Once the Western Mooring iced over on January 23, 2009, it remained consistently ice-covered through April 6 – a period of 73 days. The Central Mooring was also ice-covered for a substantial portion of the winter, although for a shorter duration than the Western Mooring. The Central Mooring was ice-covered for a period of 64 days, from January 27 to April 1. Ice cover at the Central Mooring was also less consistent, with the percent of local ice cover dropping below 100% on several occasions throughout the

winter season. The Eastern Mooring received only sporadic ice cover, which occurred toward the end of winter, between March 2 and March 21. During this 19-day period, local ice cover at the Eastern Mooring dropped to 0% on three occasions.

## 4.4 Other Observations of Physical Phenomena

### 4.4.1 Near-inertial Oscillations

Currents in the open waters of Lake Superior are dominated by near-inertial energy (Austin 2013). These near-inertial oscillations have a period of approximately 16.0-16.5 hours, depending on the latitudinal position within the lake, and occur along the thermocline, where there is a density interface between the less dense water of the epilimnion and the denser waters of hypolimnion. This phenomenon is observed in the thermistor data, causing fluctuations in thermocline depth of about 5 to 10 meters over this 16.0-16.5 hour period (Figure 17). The presence of near-inertial observations is corroborated by ADCP data from moorings, and is discussed in detail in Austin 2013.

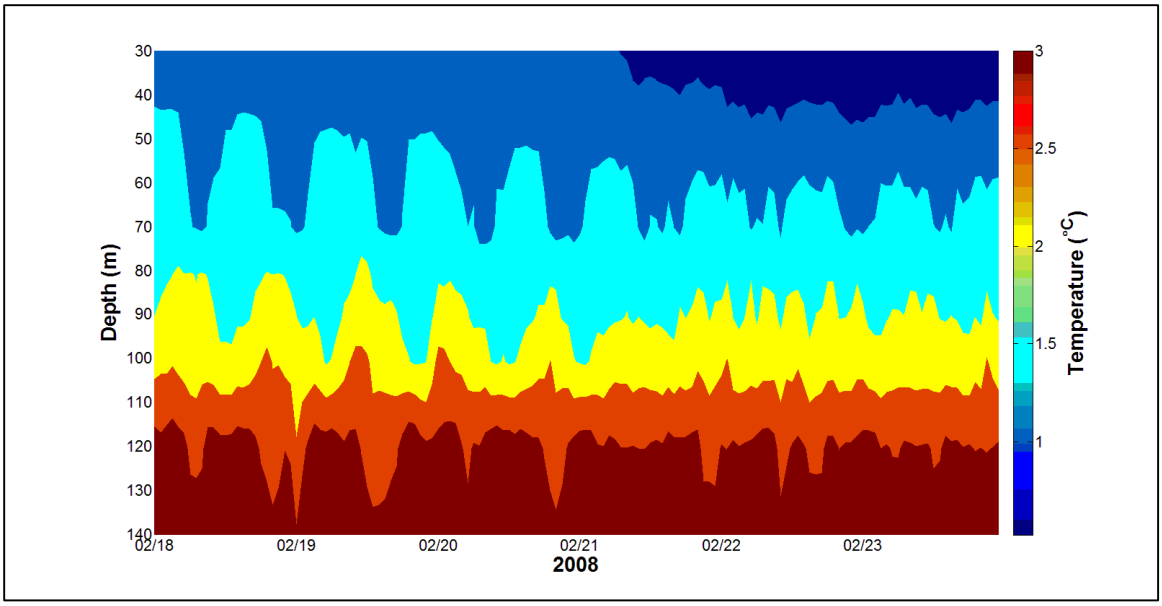


**Figure 17. Near-inertial Oscillations at Western Mooring.** Near-inertial oscillations are observed in the thermistor data during periods of stratification. Presented here is an example of these oscillations during a period of negative stratification in the winter. Oscillations are observed through fluctuations in thermocline depth, with a period of approximately 16 hours.

# 5.0 Discussion

## 5.1 The Effect of Ice Cover on Winter Heat Flux

A reasonable assumption would be that years with colder-than-average meteorological conditions would be correlated with years of above average ice cover. It is less straightforward to predict how heat fluxes would respond to these seasons of cold air temperatures and high ice cover. As discussed in Section 2.3, cold air temperatures have the potential to drive equilibrative heat flux terms more negative, and ice cover can reduce the heat input from shortwave radiation through increased albedo. These effects would result in more negative heat flux from the lake throughout the winter, and thus a colder winter water column. However, ice cover creates a barrier at the lake-atmosphere boundary layer, thereby insulating the lake surface from the overlying atmosphere. This has the potential to inhibit heat loss and "lock-in" heat at an ice-covered location for the duration of the ice-covered season.

Because high-ice years are also expected to be years with below average air temperatures, the tendency of cold air temperatures to increase heat loss from the lake may, in effect, be competing with the tendency of ice cover to insulate the lake from this heat loss. While an increase in heat loss from water body due to colder meteorological conditions can be reasonably predicted, much less is known about a lake's thermal response to ice cover. It is likely that ice-cover is a source of interannual variability in a lake's thermal structure; however, due to the scarcity of lake temperature data available from ice-covered lakes, these mechanisms are not well-characterized.

In order to investigate the effects of ice cover on the thermal characteristics of the lake, we can examine the behavior of the lake during the icy winter of 2009. With both mooring thermistor data and local ice cover data available throughout this winter at sub-daily and daily resolution, respectively, the extent and manner to which ice cover influences the underlying water column can be analyzed at relatively high temporal resolution. Additionally, because the moorings are deployed year-round, we are not only able to examine the ways in which winter meteorological conditions and ice are manifested in the lake's thermal structure in a short-term context, but also whether these winter conditions have any effect on the following summer. This is discussed in detail in Section 5.2.

The presence of the three core moorings, each with varying degrees of ice cover throughout the winter (see Figure 16), facilitates the characterization of these effects across multiple points throughout the lake, and will provide some insight into the extent to which spatial variability can occur within the lake. Each mooring represents a single point in the lake, but incoming heat energy at any given location in the lake must mix with its surroundings along some horizontal gradient. The radius around each mooring along which such horizontal mixing is important is unknown. While the spatial coverage of the mooring array is insufficient to precisely define such a distance scale, analyzing the effects of ice cover across the three core moorings will allow us to determine whether thermal structure and any influence ice has on it varies across distinct lake basins.

### 5.1.1 Heat Content

Heat content (H) is used to quantify the total amount of heat energy within the water column. While plots of raw thermistor data, such as Figure 6, are useful for visualizing the extent of positive or negative stratification, heat content is a more concise and useful metric when comparing temperature data to ice data. The time derivate of heat content (dH/dt) is particularly useful, because it represents heat flux within the water column.

Heat content must be calculated relative to a given temperature. Here, it is calculated relative to a 4°C (approximately $T_{MD}$), which is a convenient choice for freshwater lakes, because it defines heat content as zero when the lake is isothermal at $T_{MD}$. This is approximately the temperature of maximum density of water, so as water at the surface warms further, it becomes less dense than the $T_{MD}$ water below, and leads to stratification. Using this convention, heat content provides some insight as to whether the lake is experiencing a period of positive or negative stratification (heat content above or below zero, respectively). Furthermore, defining heat content relative to $T_{MD}$ makes heat content a useful proxy for estimating stratification times. When heat content is rising during the spring, the time at which the heat content crosses the threshold of zero represents the time at which the water column warmed above $T_{MD}$ and, thus, the time at which the water column began to stratify. Note that the rate of change of heat content (dH/dt), which is often the parameter of interest, does not depend on the temperature used to calculate heat content.

Heat content is calculated using the following formula:

$$H = \int \rho_w c_p [T(z) - 4°\mathrm{C}] dz \qquad \text{Equation 5}$$

Where:

- H is the heat content of the water column, relative to $T_{MD}$ ($J \cdot m^{-2}$)
- $\rho_w$ Is the density of water (in $kg \cdot m^{-3}$)
- $c_p$ is the heat capacity of water (4180 $J \cdot kg^{-1} \cdot K^{-1}$)
- T(z) is the temperature of the water at depth z (in °C)

Heat content was calculated at mooring locations over the study period for times for which there was sufficient data. The most common data deficiency, with respect to calculating heat content data, is a lack of summer surface temperature data. Because mooring thermistor strings do not extend to the lake surface, surface temperatures must be estimated. During the winter months, when stratification is weak, the uppermost thermistor provides a reasonable estimate of surface temperature. Summer surface temperatures at the Western, Central, and Eastern Moorings can be estimated based on NDBC temperature data taken from approximately 1-meter depth, because these core moorings and NDBC buoys are co-located.

There are occasionally gaps in heat content calculations at the beginning or end of the summer stratified season, when the water column is stratified, but the buoys are either not yet deployed, or have already been recovered for the winter. In 2007, there is no NDBC surface temperature data from the buoy co-located with the Western Mooring, so Western Mooring summer heat content cannot be calculated during that year. Summer heat content also cannot be calculated at the Far Western, Northern, Southern, and Far

Eastern Moorings, because there is currently no source of summer surface temperature data at these locations. However, because the uppermost thermistor can be used to estimate winter surface temperature, winter heat content can be calculated at all mooring locations.

Calculating heat content using discrete data points, such as this thermistor data, presents challenges. There is inherent uncertainty, due to not knowing the shape of the temperature profile between thermistors. Since temperature is not available as a continuous function of depth, the water column must be divided into individual depth layers for each thermistor, the heat content of each of these layers calculated, and the heat content of all layers summed to find the heat content of the water column. Using this approach, the heat content formula from Equation 5 becomes:

$$H = \sum_{\mathrm{i=1}}^{\mathrm{n_{thermistors}}} \rho_w c_p [T(z)_i - 4°\mathrm{C}] \Delta \mathrm{z_i} \qquad \text{Equation 6}$$

In estimating the heat content using Equation 6, depth layers were defined such that thermistors were centered within them, and the assumption was made that the temperature of that depth layer is determined by the temperature of the thermistor it includes. In order to determine the potential error associated with this assumption, minimum and maximum heat contents were also calculated. This was done by defining depth layers such that the thermistors form their boundaries, and assuming that the temperature of each depth layer is defined by its lower and upper thermistors, respectively (Figure 18).

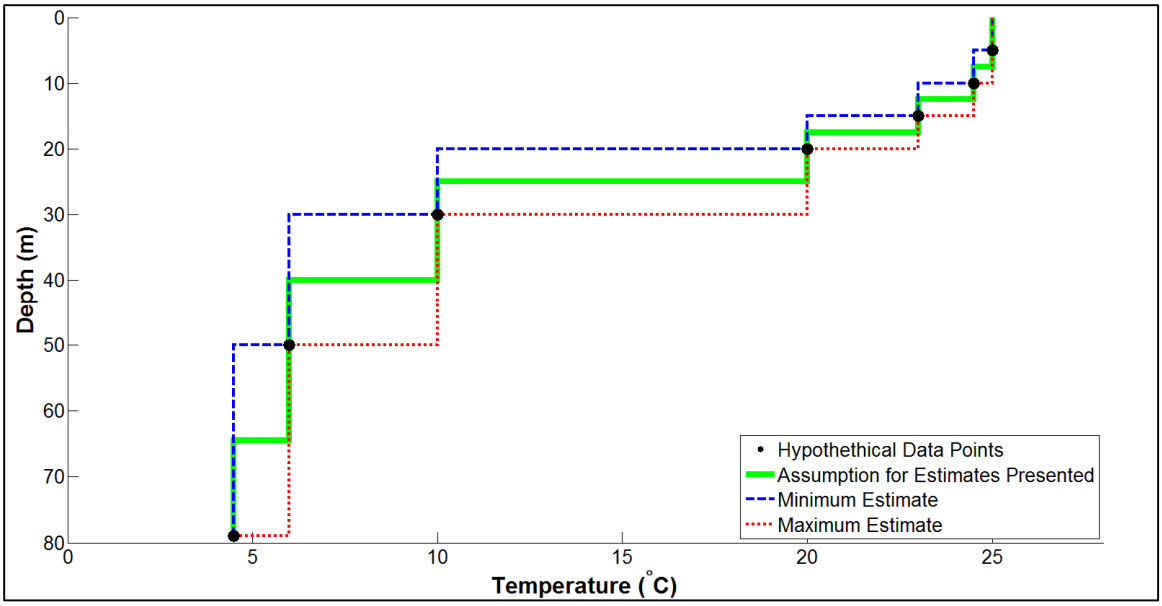


**Figure 18. Assumptions for Heat Content Estimates.** A hypothetical temperature profile is shown, to demonstrate the assumptions made when calculating heat content, as well as the way in which minimum and maximum estimates of heat content were made.

The latent heat associated with ice formation and melting was not considered in these analyses. It is minimal, relative to the fluctuations in heat content occurring within the water column. The amount of energy associated with the freezing or thawing of one meter of ice is approximately 3 x $10^8$ J·$m^{-2}$, while interannual and spatial variability in heat content is on the order of $10^9$ J·$m^{-2}$. Although no ice thickness data has been analyzed in this study, it is unlikely that open-water ice thickness is on the order of a meter. More likely, open-water ice thickness is on the order of centimeters, making the latent heat of ice formation a negligible component of the water column heat budget.

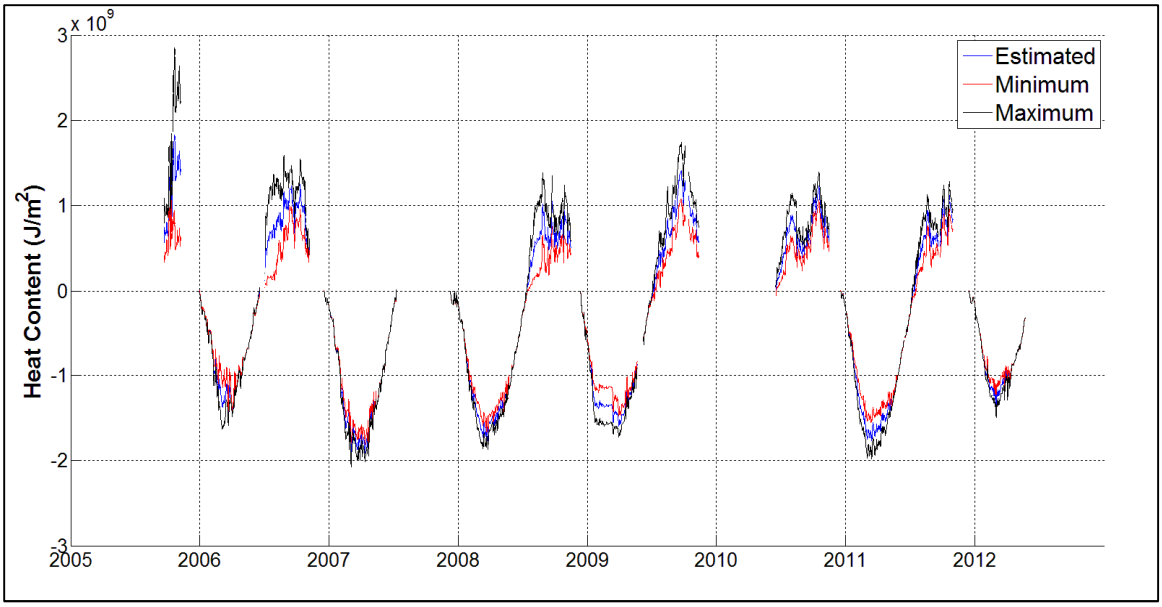


**Figure 19. Heat Content Calculation Error Range.** The range of estimated error in heat content calculation, due to uncertainty in the water column's thermal structure inherent to discreet measurements, is shown for the Western Mooring.

This estimated error range in heat content calculations, due to the assumptions discussed above, is presented in Figure 19 for the Western Mooring. Unsurprisingly, there is a greater potential for error during periods of positive and negative stratification, and virtually no potential for error due to these assumptions during the mixed periods, when the water column is approximately isothermal. The error range is exceptionally high in the 2005 summer data, due to limited depth coverage during that initial deployment, so heat content estimates from summer 2005 will not henceforth be used.

An additional issue with calculating heat content from discrete data points is that fluctuations in the thermocline can produce fluctuations in heat content. When the thermocline passes above or below a thermistor, the calculated heat content may dramatically decrease or increase in the summer, and vice-versa in the winter. This issue becomes more significant in the deeper portions of the water column, where the distance

between thermistors is greater, because each thermistor represents a more significant portion of the water column. Due to this principle, near-inertial oscillations in the lake, which result in significant fluctuations in thermocline depth (see Section 4.4.1), produce fluctuations in heat content at the near-inertial frequency. Because of this, all heat content data presented in the paper was filtered using the PL64 low-pass filter technique (Beardsly et al. 1985). This filters energy corresponding to periods below 40-hours, thereby eliminating the fluctuations imposed by near-inertial oscillations.

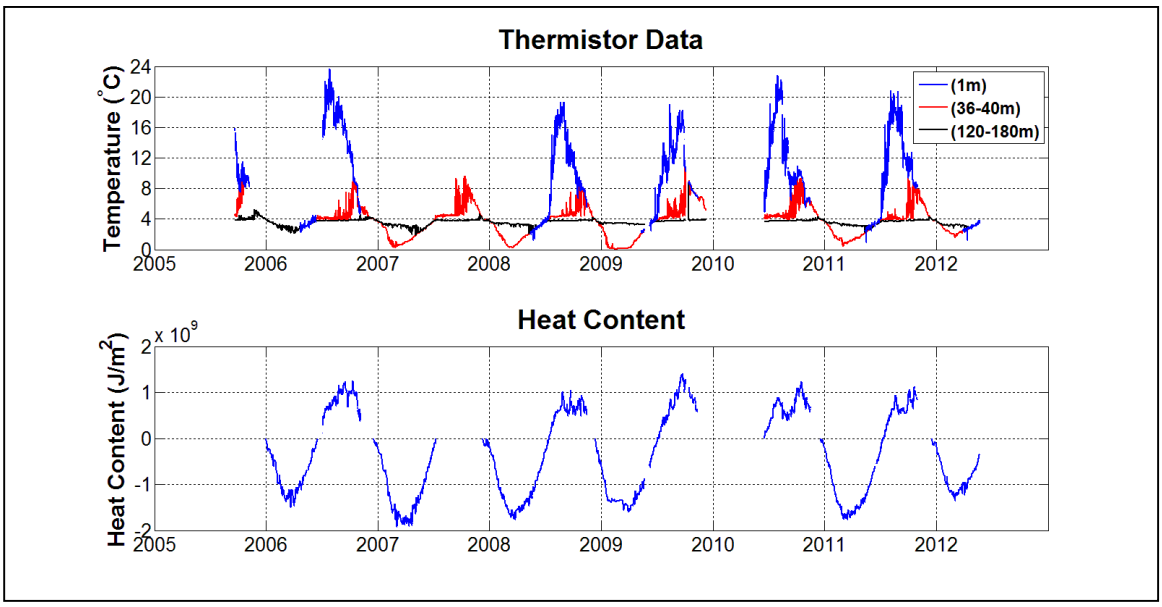


**Figure 20. Western Mooring Heat Content.** Heat content was calculated from mooring thermistor data when sufficient data was available.

Bennett (1978) describes the heat budget of Lake Superior in terms of both its "spring heat income" and its "annual heat income." The spring heat income is the amount of heat gained from the point of minimum heat content in the winter to the point at which the water column begins to stratify in the summer. Because heat content was calculated relative to 4°C here, the lake will begin to stratify when heat content is

approximately zero, because this represents a water column with a temperature of approximately $T_{MD}$.

The average annual heat content cycle was calculated at the Western Mooring, based on the complete history of thermistor data at that mooring. This was done using a Levenberg-Marquardt non-linear least squares approach to solve for coefficients to the equation with form:

$$H = C_1 + C_2 \cdot cos\left(\frac{2\pi}{1\ year} \cdot t + \varphi\right) \quad \text{(Equation 7)}$$

Where:

- H is the heat content of the water column ($J \cdot m^{-2}$)
- t is the time (units of years)
- $C_{1,2}$ are the fitting coefficients describing the annual heat content cycle ($J \cdot m^{-2}$)
- φ is a fitted phase angle

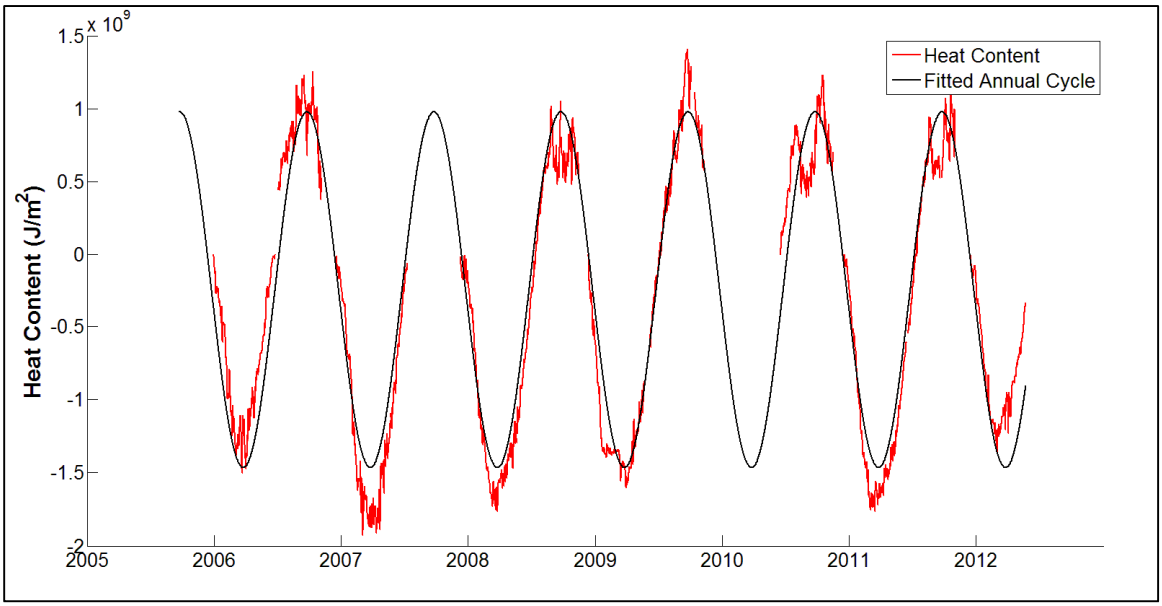


**Figure 21. Average Annual Heat Content Cycle.** The annual average heat content cycle of Lake Superior was estimated using a non-linear least squares approach.

Based on this calculated average heat content cycle, the water column at the Western Mooring reaches an average annual minimum heat content of -1.5 x $10^9$ J·m$^{-2}$, and an average annual maximum heat content of 9.8 x $10^8$ J·m$^{-2}$. Therefore, using Bennett's definitions, the water column has a spring heat income of 1.5 x $10^9$ J·m$^{-2}$, and an annual heat income of 2.4 x $10^9$ J·m$^{-2}$. These are similar to the values estimated by Bennett for Lake Superior. Bennett estimated a spring heat income between 3-4 x $10^4$ cal·cm$^{-2}$ (1.3-1.7 x $10^9$ J·m$^{-2}$) and an annual heat income between 6-7 x $10^4$ cal·cm$^{-2}$ (2.5-2.9 x $10^9$ J·m$^{-2}$).

### 5.1.2 Ice Cover as a Source of Spatial Variability in Heat Content

By analyzing mooring heat content time series in concert with local ice cover data, it is clear that ice cover does, in fact, influence heat flux (Figure 22). This effect is most dramatic at the Western Mooring. Prior to ice formation, heat content is dropping at a relatively fast rate, indicating that a substantial amount of heat is being lost from the lake. However, once ice forms, heat content remains relatively constant throughout the remainder of the ice covered season. At the Central Mooring, where ice cover is less consistent and of a shorter duration, a similar effect is observed, but is less pronounced than at the Western Mooring. The water column at the Central Mooring continues to lose heat after ice forms, but at a significantly reduced rate. Heat flux appears uninhibited at the Eastern Mooring, where ice cover was brief and sporadic; heat content continued to drop throughout the winter season, without any discernible reduction in the rate of heat loss.

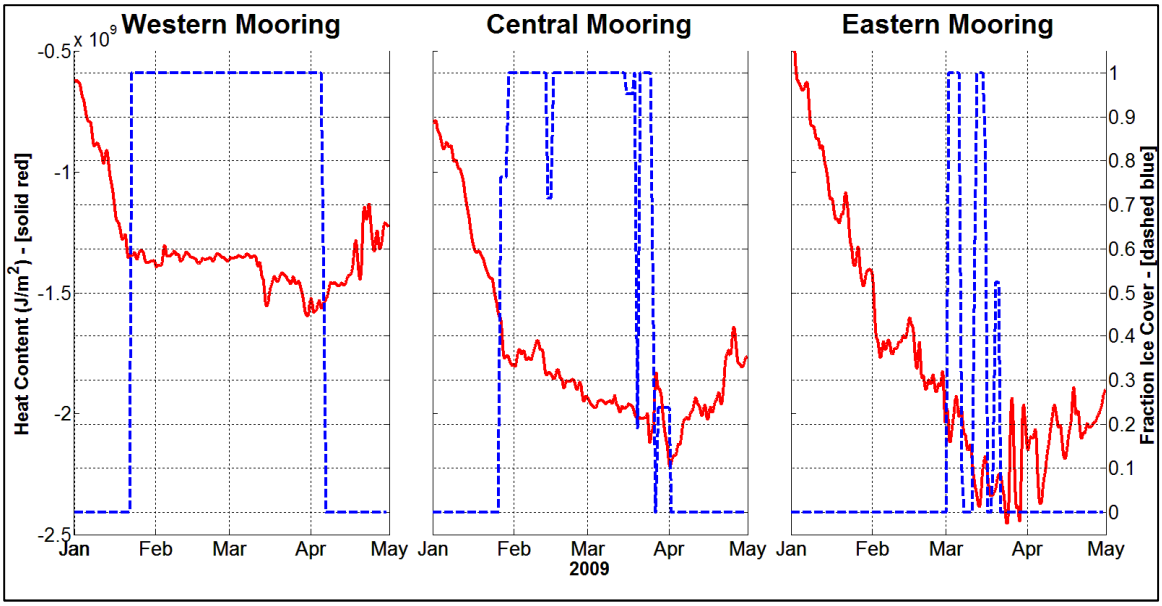


**Figure 22. Influence of Ice Cover on Heat Flux.** Heat content time-series (solid) are presented alongside local ice-cover time-series (dashed) for the Western, Central, and Eastern Moorings during the winter of 2009.

To quantify this relationship, rates of heat flux were calculated both prior to and after ice formation. This was done using a linear regression to calculate the average heat flux for the four weeks preceding and following the date of first ice formation at each of the three mooring locations (Figure 23). At the Western Mooring, heat flux prior to ice formation was -343 ± 3 $W \cdot m^{-2}$. After ice formed, heat flux was reduced to -3 ± 11 $W \cdot m^{-2}$. This represents a heat flux reduction of more than 99%. At the Central Mooring, heat flux went from -336 ± 4 $W \cdot m^{-2}$ pre-ice to -63 ± 9 $W \cdot m^{-2}$ post-ice, a reduction of approximate 81%. At the Eastern Mooring, heat flux was calculated to be -106 ± 15 $W \cdot m^{-2}$ before ice, and -124 ± 20 $W \cdot m^{-2}$ after ice, a change that is within the error bars of the estimate. These changes in heat flux observed before and ice formation cannot necessarily be attributed entirely to ice, as meteorological conditions and timing within the annual shortwave radiation cycle would also influence these rates. However, the dramatic and statistically significant reductions observed at the Western and Central

Moorings, occurring at the time of local ice formation, demonstrates that ice must have an important influence on heat flux between the lake and the atmosphere.

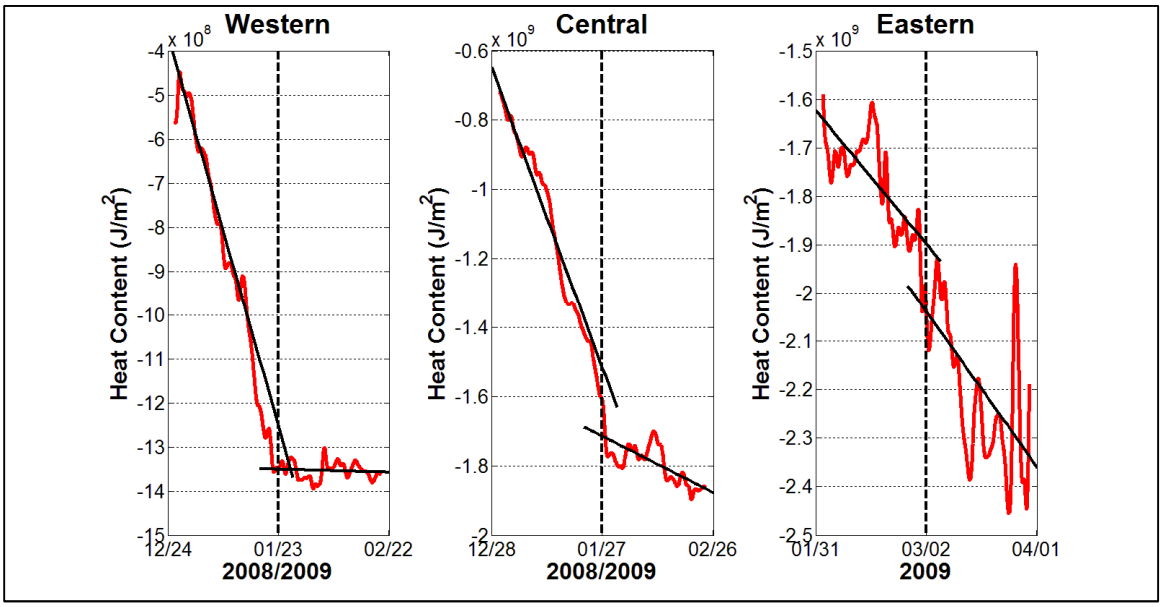


**Figure 23. Heat Flux Before and After Ice Formation.** Heat content is shown at each of the three core mooring locations for a 28-day period preceding and following the date of first ice formation (dashed vertical line). Average pre- and post- ice heat flux was calculated as the slope of the heat content line over the 28-day period before and after the first day on which ice was present around the mooring.

Further, these effects are expressed on local scales, as opposed to a lakewide scale, as demonstrated by the varying rates of heat loss among moorings, which corresponds with their spatially varying amounts of ice cover. Ice cover in the western basin of the lake, for instance, does not have any significant effect on the rate at which heat is lost in the eastern basin. This suggests that any horizontal mixing occurring within the lake is on scales much smaller than the size of the lake over timescales of a few months.

This holds true throughout the duration of the ice-cover season, as these local variations in heat content are not mixed away over the course of the winter. The Western Mooring, which experienced a reduction of heat flux to near zero, had a

significantly higher heat content at the end of the winter season than did the Central or Eastern Moorings, which both continued to experience some level of heat loss throughout the winter. The Central Mooring, which experienced a significantly reduced heat flux in the presence of ice cover, had a slightly higher heat content at the end of the winter than the Eastern Mooring. Therefore, any ice-driven spatial variation in heat content at these basin-sized scales will ultimately result in spatial variation in the end-of-winter heat content.

While this analysis clearly demonstrates the existence of a relationship between ice cover and heat flux, the details of this relationship cannot be fully discerned. Perhaps the most substantial deficiency is the lack of data from years of high ice cover. As discussed in Section 4.3, 2009 is the only year during the study period during which there was considerable open-water ice cover. Additional thermistor data from any future years with high ice cover will be valuable in corroborating these results and better characterizing the way in which ice influences heat flux.

For instance, the timing of ice cover is likely to be important. Ice that is present during periods of extreme cooling is expected to have a greater impact on heat content than ice present during periods when the lake is closer to being in equilibrium with its surroundings. This is simply because if ice halts heat flux during periods when heat loss is otherwise near its annual peak rate, the amount of heat retained within the water column is greater that would be lost in the absence of ice is greater. Additionally, if ice were to thaw particularly late in some years or at some locations, after which heat content had reached its annual minimum, ice cover could inhibit spring warming instead of

winter cooling. With only one year of under-ice data, we are unable to verify these hypotheses. These, however, are some of the questions that data from additional high-ice years would be helpful in investigating.

Further, to precisely characterize this correlation between ice cover and heat flux, higher-resolution ice data would be necessary. Gerbush et al. (2008) examined the relationship between heat flux and ice cover on Lake Erie, using high-resolution data from flight transects. They demonstrate that the relationship between ice cover and heat flux is different when analyzed at spatial resolutions of 1.2 km, 2.4 km, and 3.6 km. Further, their results show a non-linear relationship between heat flux and ice cover, and find that sensible heat flux is essentially uninhibited by ice cover at ice concentrations below about 70%.

Although the 4-km (16 $km^2$) spatial resolution of the ice data used in this analysis is a high-resolution dataset by current standards, the results of Gerbush et al. (2008) suggest there are details that it is incapable of capturing. Since ice cover data used in this analysis shows only the presence or absence of ice at each 4-km grid point, there is no way to discern the magnitude of ice cover at each location, in terms of ice thickness or the percentage of coverage within a given grid point. Specifically, some 4-km grid points that show ice cover, as opposed to water, may be mostly, but not completely, ice covered. Because the percentage of ice cover is likely important on scales much smaller than 4-km, we cannot establish a quantitative correlation between the percentage of ice cover and the extent to which heat flux is inhibited. Such analysis would require ice data on higher-resolution, micro-meteorological scales.

Understanding the mechanisms underlying the correlation, however, is not the goal of this analysis. Rather, we are able to demonstrate that ice cover can inhibit heat flux. This is important because it shows that cold meteorological conditions may not always result in a cold water column. When those cold meteorological conditions result in ice cover, the opposite can be true. By creating a barrier between the lake and the overlying atmosphere, ice can prevent the lake from cooling, and result in a warmer water column, as was the case in 2009. Under large lakes that receive spatially variable ice cover, such as Lake Superior, this effect of ice cover on winter heat flux is a source of spatial variability in end-of-winter heat content.

## 5.2 End-of-Winter Heat Content as a Predictor of Stratification Onset

Between the winter and summer stratified seasons, the water column mixes completely and warms isothermally. Once this isothermal water column reaches a temperature near $T_{MD}$, the water column begins to stratify. Two parameters that are inherently important in determining the time at which the water column will stratify are the initial heat content from which the water column must warm and the rate at which the water column warms. When the water column is warming from a lower initial ("end-of-winter") heat content, a reasonable assumption would be that it would take longer to warm to $T_{MD}$ than for a water column that starts with a higher initial heat content, resulting in later stratification for the colder water column. Likewise, a reasonable assumption would be that a faster warming rate would result in an earlier stratification time than a slower warming rate.

However, the temperature of the water column and the rate at which it warms are not independent. Based on the heat flux equations presented in Section 2.3, a cooler water column would warm at a faster rate than a warmer water column, assuming all other factors are equal, due to the equilibrative components of heat flux. The magnitude of these terms depends on the temperature difference between the lake surface and the overlying atmosphere, amongst other factors. During a warming period, when the water column is isothermal, the surface temperature is the same as the temperature throughout the water column. Therefore, the air-water temperature difference would be greater for a colder water column than a warmer water column, leading to greater equilibrative heat flux and, thus, a faster warming rate. The magnitude of the remaining heat flux term, shortwave radiation, is independent of air and water temperatures.

Given that colder water columns result in faster warming rates, this spring warming is a process that has the potential to diminish, over time, variability in heat content from winter months. That is, some of the variability in winter heat content is inevitably "lost" during spring warming, because a more negative heat content will result in a more positive heat flux, allowing cold springs with low heat content to "catch up" with warmer years or locations. However, the relative significance of the variability in heat content compared to the variability of spring warming rates will ultimately determine the extent to which winter variability is preserved. The thermistor datasets from the mooring array provide an excellent opportunity to examine the extent to which winter variability influences the timing of stratification, as opposed to being lost from the temperature record during spring warming.

As discussed in Section 5.1.2, ice-driven variability in heat flux resulted in significant variability in end-of-winter heat content at the three core moorings. Ice cover during the winter of 2009 prevented the Western Mooring from cooling to the extent of the other moorings, and the Western Mooring has a higher heat content than these moorings at the end of the winter season. For reasons discussed above, an initial hypothesis, then, would be that the Western Mooring will warm at a slower rate than the other two moorings. However, the question remains as to whether any variability in warming rates is sufficient to counter the significant variability in end-of-winter heat content.

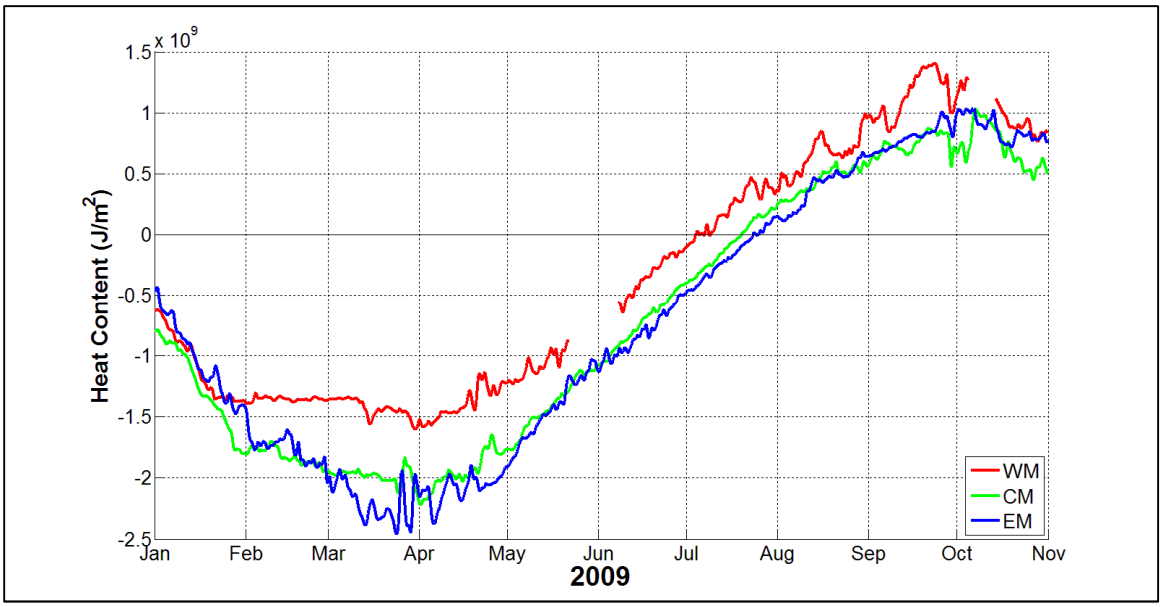


**Figure 24. Heat Content at Core Moorings, 2009.** Heat content time-series are shown for the core moorings, beginning in the winter of 2009 and continuing through the following spring and summer.

By plotting heat content from the three core moorings in 2009 from winter through the following summer, it is clear that during that year, some of the winter spatial variability is preserved within the temperature record through the spring warming period

(Figure 24). As a result, this spatial variability from the winter season did, in fact, influence the timing of stratification during the following summer.

Because heat content was calculated relative to 4°C, a heat content of zero represents a water column with a temperature of approximate $T_{MD}$. As such, the time at which heat content reaches zero can be used as a proxy to estimate the time at which the water column will begin to stratify. These data show that because Western Mooring had a "head start" in the spring warming process, due to higher end-of-winter heat content, it ultimately stratified significantly earlier than the other two core moorings. This means that the variability in warming rates at the core moorings in 2009 was insufficient to counter the variability in end-of-winter heat content.

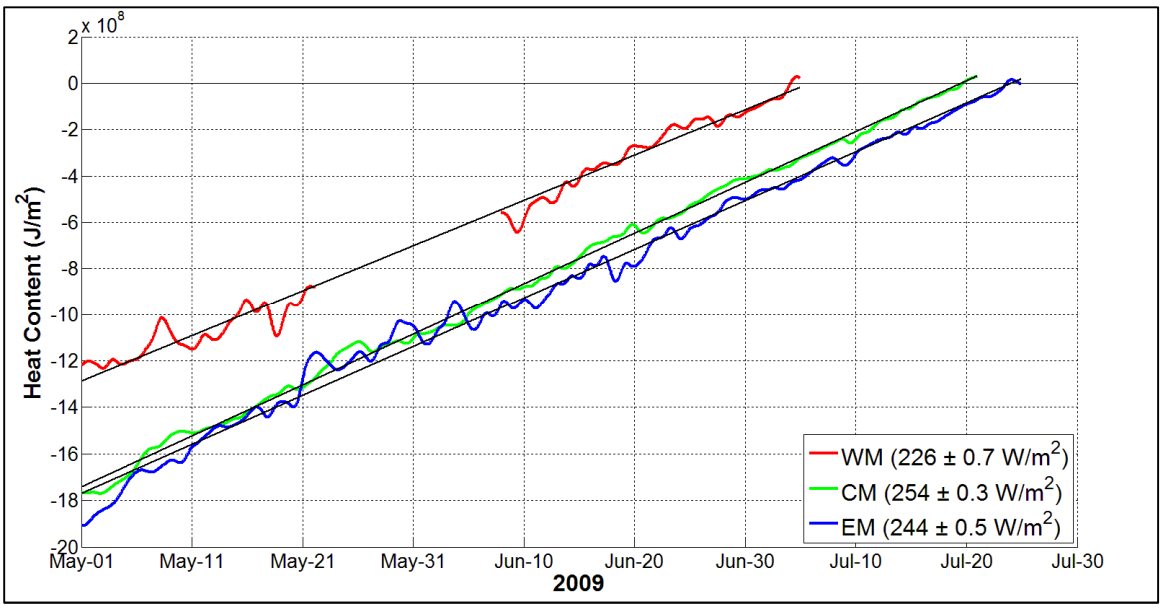


**Figure 25. Spring Warming Rates at Core Moorings in 2009.** Spring warming rates are shown for the three core moorings during the spring of 2009. Warming rates were calculated beginning May 1 through the time at which the heat content reached zero (a proxy for summer stratification onset).

Taking a closer look at the 2009 spring warming period (Figure 25), all three core moorings warm at a similar rate, despite varying water column temperatures. There is

some variability in warming rates, and this variability may be, in part, attributable to temperature differences in the water column. The Western Mooring, with the warmest water column, is warming slightly more slowly (226 W/m$^2$) than the Central and Eastern Moorings (254 W/m$^2$ and 244 W/m$^2$, respectively), which have colder water columns. This variation, however, is insufficient to overcome the variability in end-of-winter heat content, over the length of the warming period. The Western Mooring does, in fact, stratify significantly earlier than the other two core moorings in 2009. The Western Mooring had warmed to a heat content of zero by July 5, while the Central and Eastern Moorings did not reach a heat content of zero until July 21 and July 25, respectively. Based on this proxy, the Western Mooring began its summer stratified season more than two weeks earlier than either of the other two moorings.

Thermistor data from the Western Mooring provides an opportunity to examine interannual variation in spring warming rates. Heat content can be calculated for the Western Mooring spring warming period during five different years, allowing for comparison of spring warming rates over multiple years at a single location.

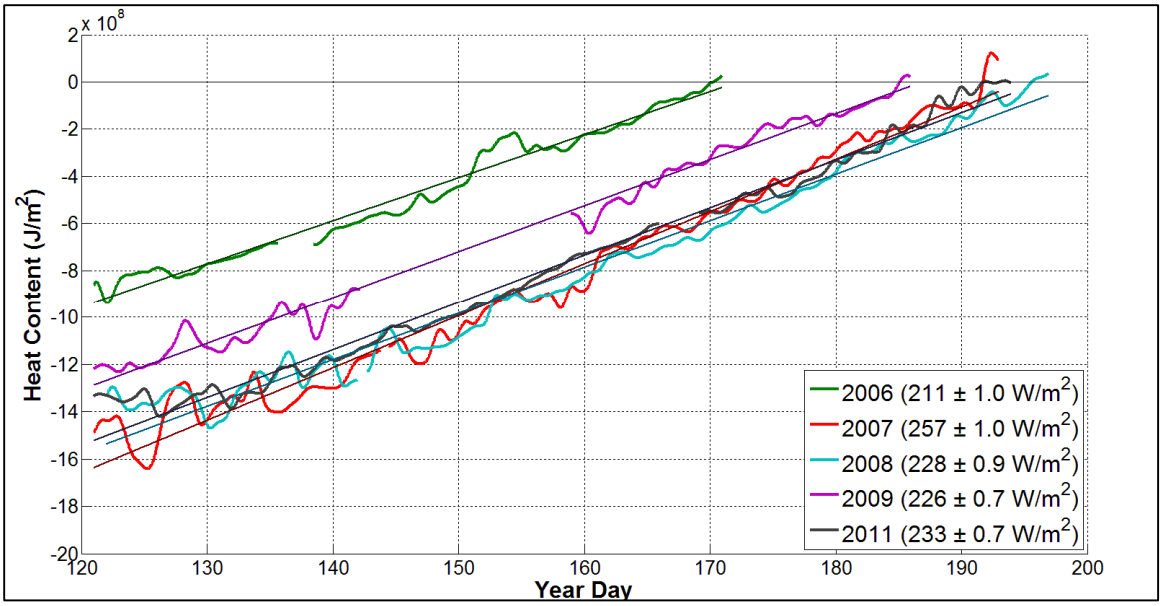


**Figure 26. Spring Warming Rates at the Western Mooring over Multiple Years.** Interannual variability in spring warming rates at the Western Mooring over the study period is shown, and the rates for each year are listed in the figure's legend.

A similar analysis was conducted using multiple years of data from the Western Mooring, in order to assess interannual variability in warming rates (Figure 26). As with the analysis of spring warming rates at the core moorings in 2009, the variability in warming rates observed at the Western Mooring over multiple years may be, in part, attributable to differences in water column temperature. The year with the warmest end-of winter heat content (2006) had the slowest warming rate, at 211 W/m$^2$. The year with the coldest end-of winter heat content (2007) had that fastest warming rate, at 257 W/m$^2$. Again, however, over the duration of the spring warming period, this variability is insufficient to account for the variability in end-of-winter heat content.

For example, the water column at the Western Mooring still stratified significantly earlier in 2006 than in 2007. In 2006, the water column stratified on June 20; in 2007, it stratified 22 days later, on July 12. The higher warming rate in 2007 was insufficient to account for its significantly lower initial heat content.

These results make sense in the context of annual heat flux cycles, because shortwave radiation is the dominant heat flux component during the spring warming period. Further, shortwave radiation is independent of water column temperature, so it is of similar magnitude from year to year, with variability due primarily to variability in cloud cover. Lofgren and Zhu (2000) estimate the annual heat flux cycles for each of the five Laurentian Great Lakes, and show sensible and latent heat flux to be very small compared to the total heat flux. Their results for Lake Superior in June, for instance, estimate sensible and latent heat flux (5-15 $W \cdot m^{-2}$) comprising only 5-10% of the total heat flux (160-170 $W \cdot m^{-2}$) in the lake. The total heat flux estimates made by Lofgren and Zhu, however, are significantly lower than the actual heat flux observed in the mooring thermistor data.

Consistent with the conclusion that heat flux is dominated by shortwave radiation during the warming periods are values of clear-sky shortwave radiation calculated for the months comprising the warming period (Figure 27). During May, June, and July, clear-sky shortwave radiation ranged from approximately 350 to 405 $W \cdot m^{-2}$. This is much higher than that actual heat flux observed at the mooring locations; however, that is to be expected, since this is an estimate of the clear-sky shortwave radiation, as opposed to net shortwave radiation. A significant portion of this downwelling shortwave radiation is absorbed by cloud cover or reflected from the water surface, resulting in a lower net heat flux, such as those observed at the mooring locations.

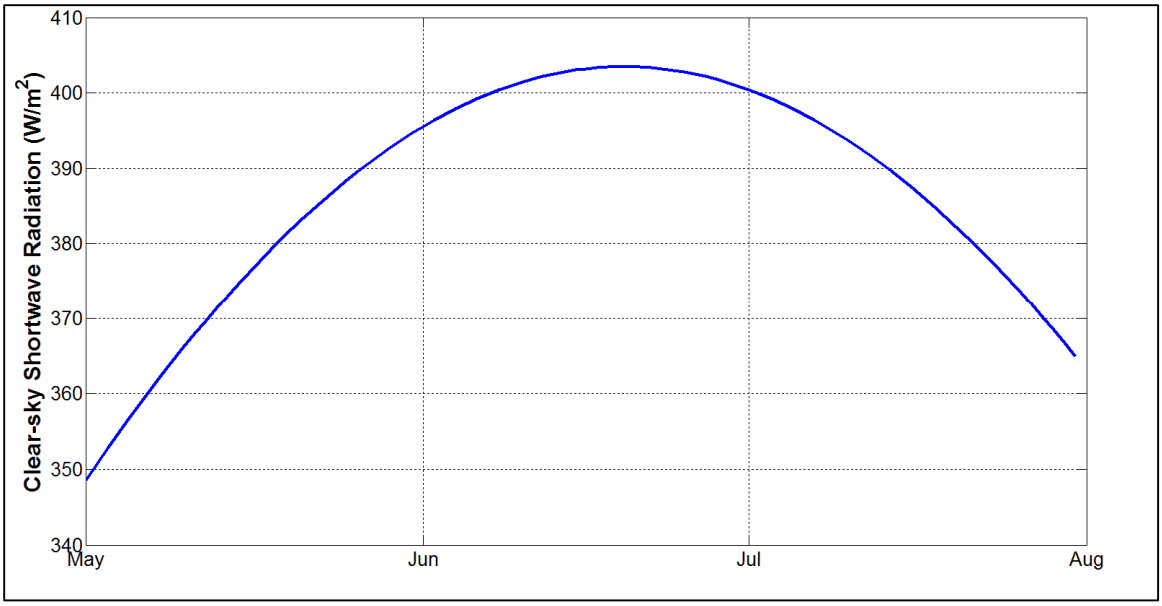


**Figure 27. Clear-sky Shortwave Radiation during Warming Period.** The clear-sky shortwave radiation is shown for May, June, and July.

The relationship between end-of-winter heat content and the timing of summer stratification holds true over multiple moorings and years. In Figure 28, a data point is plotted for each year of data available at each of the core moorings. With an $r^2$ value of 0.90 ($p<0.05$), there is an obvious and statistically significant correlation between end-of-winter heat content and the timing of the onset of summer stratification. Within this dataset, the earliest stratification time was observed in 2010, when the Eastern Mooring stratified on June 12. The latest observed stratification was at the Central Mooring in 2011, which stratified on July 26. This represents a span in stratification timing of 44 days over the course of the study period, amongst the core moorings. As such, end-of-winter heat content is shown to be a strong predictor of the timing of summer stratification over a wide range of conditions. This is consistent with the findings of Rodgers (1987), who found a correlation between winter water column temperatures and the timing of summer stratification onset in Lake Ontario.

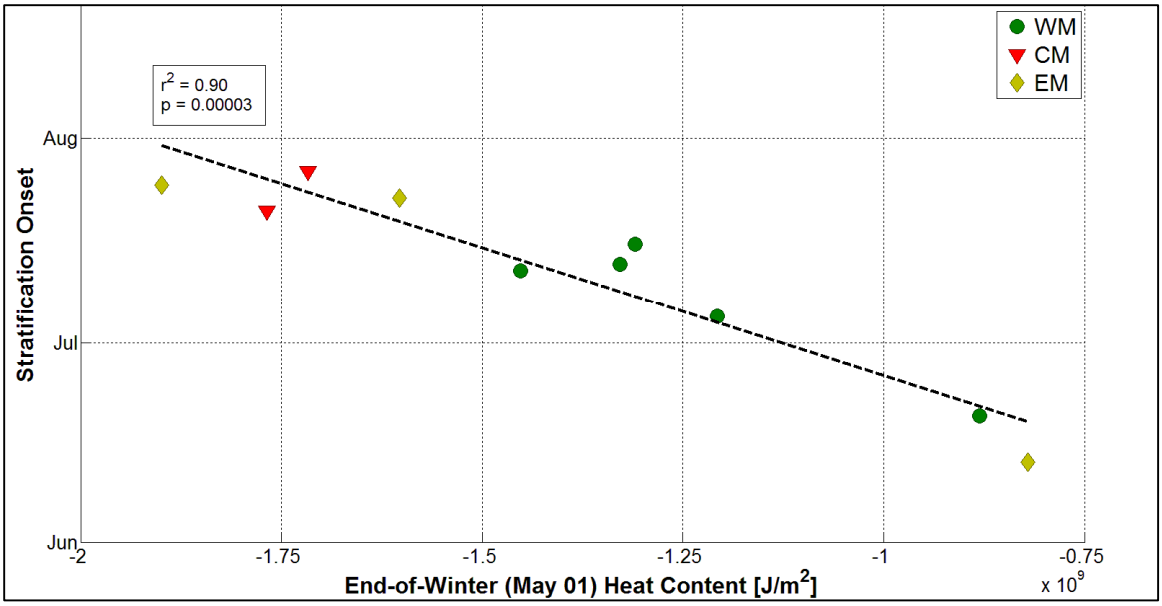


**Figure 28. Correlation between end-of-winter heat content and stratification onset time at core moorings.** A linear regression shows the correlation between end-of-winter heat content and stratification onset for the three core moorings (r=0.90, p<0.05).

The end-of-winter heat content was defined here using a consistent date of May 1, because this is a date that is early enough to produce a robust time-series for each spring warming period, but late enough that any open-lake ice has already thawed. The analysis was repeated using dates of April 1 and June 1, and the same conclusions were reached, indicating that results are not sensitive to this value. Choosing a specific date to define end-of-winter heat content has practical advantages over choosing to use a metric such as minimum heat content. If one sought to predict the time at which the water column would stratify during a given year, a single measurement would be required on May 1. Further, because the water column is isothermal during these warming periods, the measurement could be taken from any point in the water column, including the surface. In order to identify the minimum heat content, data would need to be collected throughout the entire winter season and throughout the entire water column.

While the relationship between end-of-winter heat content and stratification onset time is quite strong at the core moorings, it weakens when outer moorings are included (Figure 29). End-of-winter heat content remains an important factor in determining the time at which the water column will stratify; the $r^2$ value for this correlation is 0.60 ($p<0.05$). However, the fact that this correlation is weaker than it was when only core moorings were considered (Figure 28) suggests that other factors, in addition to end-of-winter heat content, are important in determining the timing of summer stratification onset when considering both outer and more central portions of the lake.

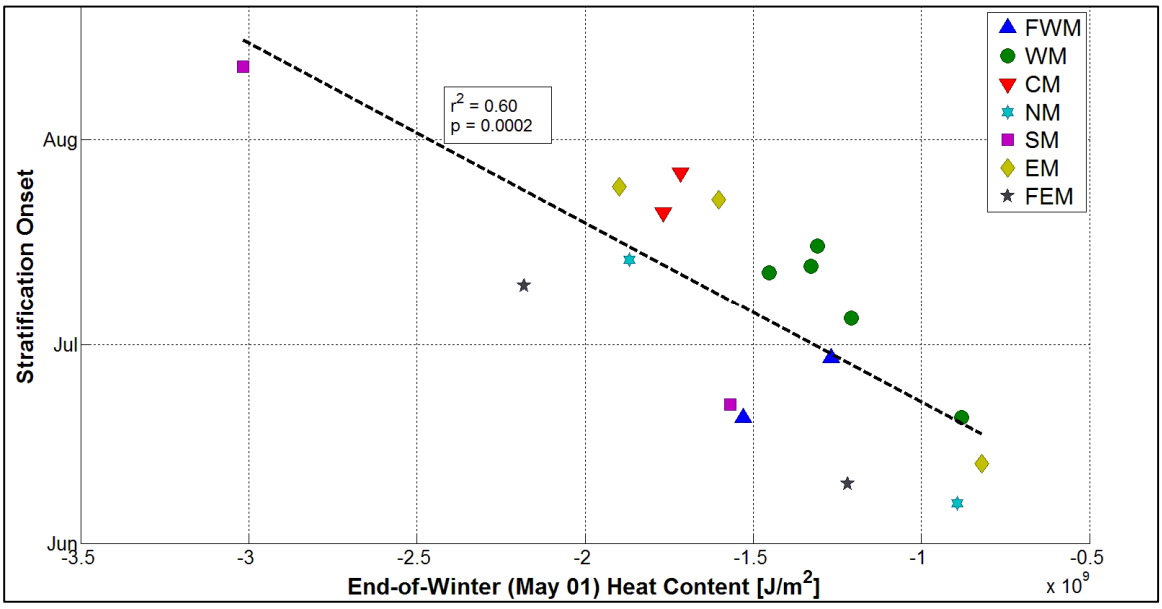


**Figure 29. Correlation between end-of-winter heat content and stratification onset time at all moorings.** A linear regression shows the correlation between end-of-winter heat content and stratification onset for all mooring locations ($r=0.60$, $p<0.05$).

The weaker correlation between end-of-winter heat content and stratification onset is due, in part, to spatial variability in warming rates (Figure 30). There is a greater amount of variability in warming rates when outer moorings are included, and this variability is no longer insignificant compared to the variability in heat content. In all years for which there is mooring thermistor data, the three core moorings warmed at rates

below 260 W/m$^2$, while the outer moorings warmed at rates above 260 W/m$^2$. In particular, the Southern Mooring, for which there is two years of data, warmed at a rate above 320 W/m$^2$ both years, and the Far Eastern Mooring, for which there is also two years of data, warmed at a rate above 350 W/m$^2$ both years.

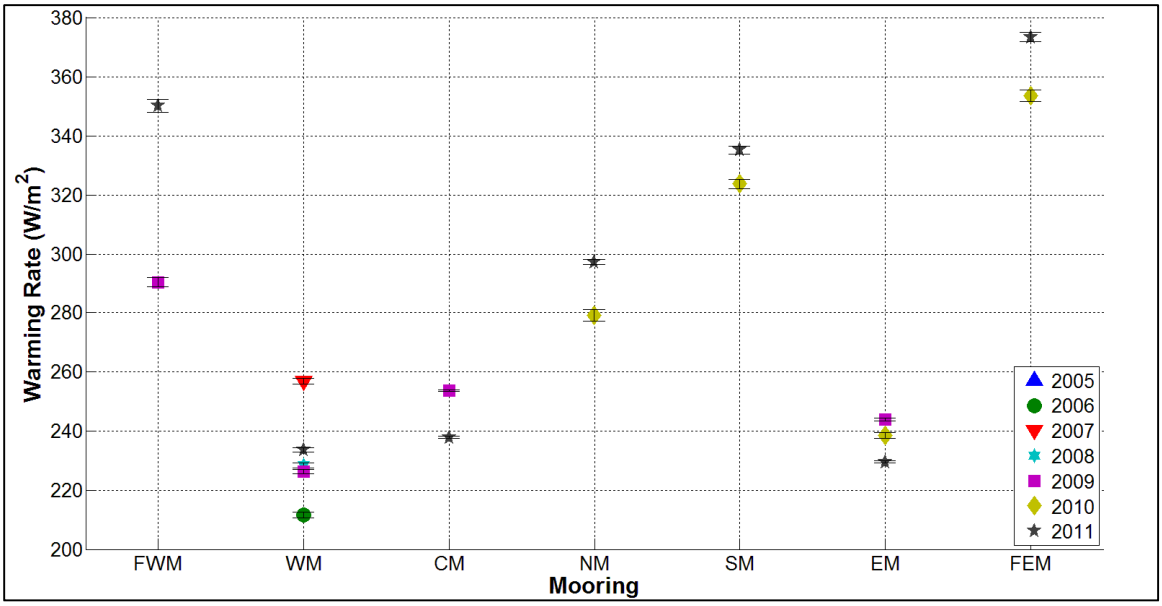


**Figure 30. Spatial Variability in Warming Rates.** One point is plotted to show the spring warming rate for each year there is data available for that mooring location.

This variability in warming rates, on the order of 100 W/m$^2$, will produce differences in heat content on the order of what is necessary to overcome the variability in end-of-winter heat content observed in the data, over the durations of spring warming observed. When considering all years and moorings for which thermistor data is available, the average length of the warming period, defined as beginning May 1 and ending when the water column stratifies, is 67 days. Over this 67 day period, a 100 W/m$^2$ difference in warming rate, for example, would result in a heat content difference of approximately 5.8 x 10$^8$ J/m$^2$. This difference is not insignificant compared to the variability in end-of-winter heat content observed (see Figure 29).

Similar spatial variability in end-of-winter heat content is not observed in the data, so the variability in warming rates must be due to something other than the initial temperature of the water column. There is also no apparent correlation between a mooring's warming rate and other potentially influential properties of the mooring location, including water column depth, distance from shore, or latitude. In addition, due to the paucity of measurements, little is known about spatial variability in over-lake air temperature, so it unknown to what extent variability in warming rates may be influenced by variability in over-lake air temperature.

Some of the spatial variability in warming rates can likely be explained through horizontal advection. For example, the Southern Mooring, which warms at a faster rate than most other locations (see Figure 30), is located in a region of exceptionally uneven bathymetry (Figure 31). Specifically, it is located in a deep valley, with depths of 350 to 400m, but is immediately surrounded by much shallower regions of 100m or less.

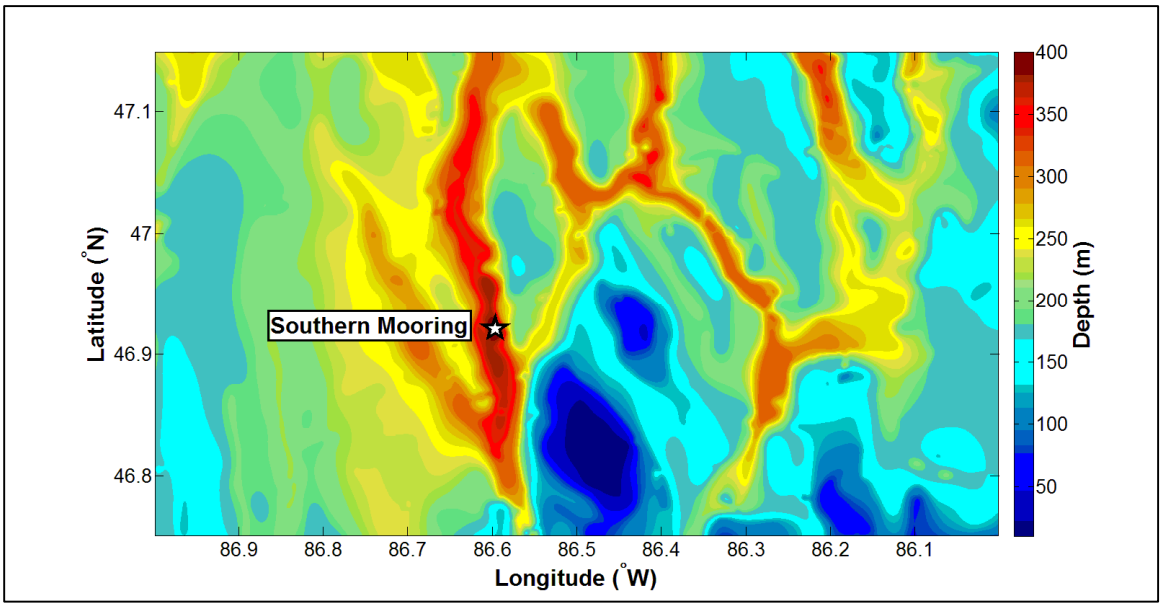


**Figure 31. Southern Mooring Bathymetry.** The bathymetry for the region surrounding the Southern Mooring is shown.

If there were no horizontal mixing, the shallower regions would warm faster than that deeper regions, resulting in a warmer water column in shallow regions and a colder water column in deeper regions. However, there must be some horizontal advection. This would explain why some moorings experience higher warming rates than others. Those locations in deep water, surrounded by shallower water, are receiving heat both from the atmosphere, and from the shallower water around them. The opposite would be true for moorings located in shallow water, but surrounded by deep water.

To examine this, we can assume that the temperature of the water column is constant within some radius of the mooring, and then calculate heat flux using the average depth within that radius. However, the distances over which such horizontal mixing may be significant is not clear, and may not be the same at all mooring locations. Therefore, the analysis was conducted using a range of averaging radii, from 0 km to 100 km (Figure 32), and was done using the year 2011, because that is the one year where all seven moorings were deployed during the spring warming period.

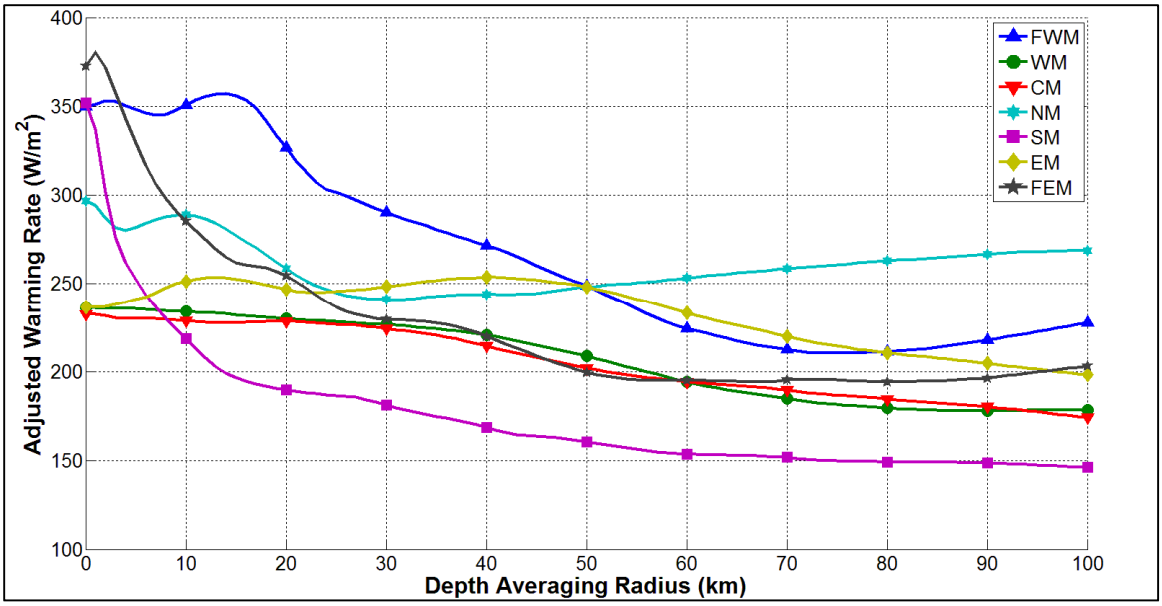


**Figure 32. Adjusted Warming Rates using Depth-Averaged Radius.** Warming rates were adjusted by assuming that the temperature of the water column within a certain radius of the mooring location is spatially constant, and then using the average depth within that radius to calculate the warming rate.

Based on these adjusted warming rates, it does appear that horizontal advection can explain some of the spatial variability in spring warming rates. Those moorings with above average warming rates are shown to warm at rates similar to other moorings when an average depth around the mooring is used, as opposed to the depth at a single mooring point. This shows that although end-of-winter heat content explains much of the variability in stratification times, it is also important to consider heat flux through horizontal advection, which is particularly important in regions of the lake with uneven bathymetry.

# 6.0 Conclusion

The mooring thermistor data presented here addresses some of the deficiencies common to modern research into the thermal structure of large lakes. Whereas many temperature datasets are biased toward summer data, are taken from a single point, or are taken only from the near-surface, temperature data from these moored thermistors is collected year round at multiple locations, and spans the entire water column. This unique dataset facilitates year-round examination of Lake Superior's thermal structure at a high temporal resolution, and provides a rare look at the winter thermal structure of a large, partially ice-covered lake.

As such, the focus of this thesis has been on Lake Superior's thermal structure during the winter months, and the mechanisms driving interannual and spatial variability in that winter thermal structure. While the water column negatively stratified every year at all mooring locations during the study period, the strength of this negative stratification varied significantly from year to year and from location to location (Figure 9).

In analyzing ice-cover data alongside the mooring thermistor data from the icy winter of 2009, ice cover was shown to inhibit heat flux. Specifically, when cold meteorological conditions resulted in significant ice cover, that ice cover inhibited heat loss, effectively "locking in" heat and producing a warmer water column. Because ice cover varies spatially across the lake, the inhibition of heat loss by ice cover can translate into ice acting as a mechanism for spatial variability in the lake's end-of-winter heat content. Such variability in end-of-winter heat content was shown to be preserved

through spring warming, and to ultimately influence the timing of summer stratification, with lower end-of-winter heat contents strongly correlated with a later onset of stratification.

While the results presented herein demonstrate that ice cover can inhibit heat flux, the relationship presented is largely qualitative, and a detailed relationship between ice cover and heat flux cannot be established with these datasets. Any thermistor data that can be collected from these moorings during years of high ice cover will be valuable in furthering our knowledge of this relationship. Such data would allow us to corroborate these results, and examine the significance of factors such as the timing ice onset, which cannot be elucidated with a single year of under-ice data. In addition, details such as ice thickness and micro-scale ice coverage are likely to be important in establishing such a relationship. As such, any future temperature and ice data collected at a higher horizontal spatial resolution will be essential toward furthering the understanding of this relationship between ice cover and heat flux.

One of the intriguing aspects of the results presented in this thesis is that they are somewhat counterintuitive in the context of recent work. Austin and Colman (2007) found that years of high ice cover are correlated with years with later summer stratification times. Here, results show that ice cover can result in a warmer water column and ultimately an earlier onset of summer stratification. It is believed that both the results of Austin and Colman (2007) and this thesis are accurate and valid. However, a way in which to reconcile the two findings is not immediately clear, and remains an important next step in this research. The answer could likely be found through a better

understanding of the spatial versus interannual effects of ice cover, because Austin and Colman examined the effects of ice cover from year to year, while the results of this thesis were reached by examining the effects of ice cover between locations.

Additional questions regarding winter thermal structure that this dataset has a potential to answer revolve around a better understanding of the intricacies dictating the onset of winter stratification and the formation of ice. During fall cooling, once the water column becomes isothermal at $T_{MD}$, it is not clear exactly what conditions will result in the onset of negative stratification, as opposed to continued isothermal cooling. Similarly, once negative stratification does form, it is not clear exactly what conditions will result in the formation of ice at the surface, as opposed to continued cooling or deepening of the epilimnion. By examining thermistor datasets alongside meteorological data, such as air temperature and wind speed records, over multiple years, some of these mechanisms may be elucidated.

The data and results presented in this thesis are significant, because they provide insight into the behavior of the lake and its response to climatic forcing during a time of year when very little is known about the structure of the water column below the surface. In addition, these results demonstrate the interconnected nature of the physical processes examined, and that conditions experienced by the lake during one season can be articulated in the lake's thermal structure in such a way that their effects extend into subsequent seasons. Here, it was specifically shown that spatial variability in heat content imposed by ice is preserved through spring and affects the timing of summer stratification. This is important, because the timing of summer stratification has

significance to biogeochemical processes, such as oxygen and nutrient distribution. Further, it is likely the variability in winter heat content may have implications even farther into the subsequent year, and that future research may be able to expand upon these findings to better characterize the lake's phenology. Understanding the mechanisms through which the lake responds to variable climatic forcing, such as the relationship between ice and heat flux presented here, will be essential to predicting how Lake Superior, and other large lakes, will respond to changes in the Earth's climate.

# 7.0 Bibliography


Assel, R.A. 2003. An Electronic Atlas of Great Lakes Ice Cover. NOAA Great Lakes Ice Atlas, Great Lakes Environmental Research Laboratory. http://www.glerl.noaa.gov/data/ice/atlas/

Assel, R.A. 2005. Great Lakes ice cover climatology update: Winters 2003, 2004, and 2005. NOAA Technical Memorandum GLERL-135. NOAA, Great Lakes Environmental Research Laboratory. http://www.glerl.noaa.gov/ftp/publications/tech_reports/glerl-135/

Austin, J.A., 2013. Observations of near-inertial energy in Lake Superior. Limnology and Oceanography, 58(2): 715-728. doi:10.4319/lo.2013.58.2.0715

Austin, J.A., J. Allen. 2011. Sensitivity of summer Lake Superior thermal structure to meteorological forcing. Limnology and Oceanography, 56(3): 1141–1154. doi:10.4319/lo.2011.56.3.1141

Austin, J. A., S.M. Colman. 2007. Lake Superior summer water temperatures are increasing more rapidly than regional air temperatures: A positive ice-albedo feedback. Geophysical Research Letters, 34(6), L06604. doi:10.1029/2006GL029021

Austin, J.A., S.M. Colman. 2008. A century of temperature variability in Lake Superior. Limnology and Oceanography; 53(6): 2724–2730. doi:10.4319/lo.2008.53.6.2724

Beardsley, R. C., R. Limeburner, L.K. Rosenfeld. 1985. CODE-2: Moored array and large scale data report. Woods Hole (MA): Woods Hole Oceanographic Institute, CODE Technical Report No. 38, WHOI Technical Report 85–35.

Bennett, E.B. 1978. Characteristics of the thermal regime of Lake Superior. Journal of Great Lakes Research, 4(3): 310–319. doi:10.1016/S0380-1330(78)72200-8

Bennington, V., G.A. McKinley, N. Kimura, C.H. Wu. 2010. The general circulation of Lake Superior: mean, variability, and trends from 1979–2006. Journal of Geophysical Research, 115(C12). doi:10.1029/2010JC006261

Chen, C. T. A., Millero, F. J. 1986. Precise thermodynamic properties for natural waters covering only the limnological range. Limnology and Oceanography, 31(3): 657-652.

Coats, R., J. Perez-Losada, G. Schladow, R. Richards, C. Goldman. 2006. The warming of lake Tahoe. Climatic change, 76(1-2): 121-148. doi:10.1007/s10584-005-9006-1

Desai, A. R., J.A. Austin, V. Bennington, G.A. McKinley. 2009. Stronger winds over a large lake in response to weakening air-to-lake temperature gradient. Nature Geoscience, 2(12): 855-858. doi:10.1038/ngeo693

Gerbush, M. R., D.A.R. Kristovich, N.F. Laird. 2008. "Mesoscale boundary layer and heat flux variations over pack ice-covered Lake Erie." Journal of Applied Meteorology and Climatology, 47(2): 668-682. doi:10.1175/2007JAMC1479.1

Hampton, S.E., E. Izmest, R. Lyubov, M.V. Moore, S.L. Katz, B. Dennis, E.A. Silow. 2008. Sixty years of environmental change in the world's largest freshwater lake–Lake Baikal, Siberia. Global Change Biology, 14(8): 1947-1958. doi:10.1111/j.1365-2486.2008.01616.x

Lewis Jr., W. M. 1983. A revised classification of lakes based on mixing. Canadian Journal of Fisheries and Aquatic Sciences, 40(10): 1779-1787. doi:10.1139/f83-207

Lofgren, B. M., Y. Zhu. 2000. "Surface energy fluxes on the Great Lakes based on satellite-observed surface temperatures 1992 to 1995." Journal of Great Lakes Research, 26(3): 305-314. doi:10.1016/S0380-1330(00)70694-0

Magnuson, J.J., D.M. Robertson, B.J. Benson, R.H. Wynne, D.M. Livingstone, T. Arai, R.A. Assel, et al. 2000. Historical trends in lake and river ice cover in the Northern Hemisphere. Science, 289(5485): 1743-1746. doi:10.1126/science.289.5485.1743

McCormick, M.J. 1996. Lake Superior water temperature data, Sault Ste. Marie, MI. 1906–1992. NOAA Technical Memorandum ERL GLERL-99.

McCormick, M. J., G.L. Fahnenstiel. 1999. Recent climatic trends in nearshore water temperatures in the St. Lawrence Great Lakes. Limnology and Oceanography, 44(3): 530-540. doi:10.4319/lo.1999.44.3.0530

NOAA National Geophysical Data Center (NGDC), U.S. Great Lakes Bathymetry, Retrieved June 18, 2013, http://www.ngdc.noaa.gov/mgg/greatlakes/greatlakes.html

NOAA/NESDIS/OSDPD/SSD. 2004. IMS Daily Northern Hemisphere Snow and Ice Analysis at 4 km and 24 km Resolution. 4-km subset. Boulder, Colorado USA: National Snow and Ice Data Center. doi:10.7265/N52R3PMC.

O'Reilly, C.M., S.R. Alin, P.D. Plisnier, A.S. Cohen, B.A. McKee. 2003. Climate change decreases aquatic ecosystem productivity of Lake Tanganyika, Africa. Nature, 424(6950): 766-768, doi:10.1038/nature01833

Payne, R.E., 1972. Albedo of the sea surface. Journal of the Atmospheric Sciences, 29(5): 959–970. doi:10.1175/1520-0469(1972)029<0959:AOTSS>2.0.CO;2

Robertson, D. M., R.A. Ragotzkie. 1990. Changes in thermal structure of moderate to large sized lakes in response to changes in air temperature. Aquatic Sciences, 52(4): 360–380, doi:10.1007/BF00879763

Rodgers, G.K. 1987. Time of onset of full thermal stratification in Lake Ontario in relation to lake temperatures in winter. Canadian Journal of Fisheries and Aquatic Sciences, 44(12): 2225-2229. doi:10.1139/f87-273

Schneider, P., S.J. Hook, R.G. Radocinski, G.K. Corlett, G.C. Hulley, S.G. Schladow, T.E. Steissberg. 2009. Satellite observations indicate rapid warming trend for lakes in California and Nevada. Geophysical Research Letters, 36(22): L22402. doi:10.1029/2009GL040846

Schneider, P., S.J. Hook. 2010. Space observations of inland water bodies show rapid surface warming since 1985, Geophysical Research Letters, 37(22): L22405. doi:10.1029/2010GL045059.

Stefan, H.G., X. Fang, M. Hondzo. 1998. Simulated climate change effects on year-round water temperatures in temperate zone lakes. Climatic Change, 40(3-4): 547–576. doi:10.1023/A:1005371600527

Verburg, P., R.E. Hecky, H. Kling. 2003. Ecological consequences of a century of warming in Lake Tanganyika. Science, 301(5632): 505–507. doi:10.1126/science.1084846

Vollmer, M.K., H.A. Bootsma, R.E. Hecky, G. Patterson, J.D. Halfman, J.M. Edmond, D.H. Eccles, R.F. Weiss. 2005. Deep-water warming trend in Lake Malawi, East Africa. Limnology and Oceanography, 50(2): 727–732. doi:10.4319/lo.2005.50.2.0727

Wang, J., Assel, R.A., Walterscheid, S., Clites, A.H., Bai, X. 2012. Great Lakes Ice Climatology Update: Winter 2006 – 2011 Description of the Digital Ice Cover Dataset. NOAA Technical Memorandum GLERL-155. NOAA, Great Lakes Environmental Research Laboratory. http://www.glerl.noaa.gov/ftp/publications/tech_reports/glerl-135/

White, B., J.A. Austin, K. Matsumoto. 2012. A three-dimensional model of Lake Superior with ice and biogeochemistry. Journal of Great Lakes Research, 38(1): 61-71. doi:10.1016/j.jglr.2011.12.006